CHAPTER 16

THE ROLE OF HIGH TEMPERATURE TRANSIENT FUEL CHANNEL BEHAVIOUR IN SAFETY ANALYSIS

P.D. Thompson, H.S. Waldman, C.L. Swift-Schultz, D. Caswell, S. Girgis
Core Behaviour Branch, Safety Analysis Department
Atomic Energy of Canada Limited, Engineering Company
Mississauga, Ontario

ABSTRACT

The investigation of fuel channel behaviour during high temperature transient conditions is an integral part of CANDU reactor safety analysis. Through the investigation of the behaviour of the fuel channel under a wide range of postulated accidents, including the very improbable, channel integrity and hence the basic effectiveness of the moderator to prevent core meltdown and loss of coolable geometry can be demonstrated. For severe accident conditions such as those resulting from loss of coolant with coincident loss of emergency core cooling (LOC/LOECC), the behaviour of the channel greatly affects heat removal. Through pressure tube deformation by either circumferential strain or sag, contact with the calandria tube can be established, thereby allowing heat to be conducted directly into the moderator. The liberation of hydrogen and heat by the high temperature oxidation of the Zircaloy in the pressure tube also affects the thermal and mechanical behaviour within each fuel channel. The amount of hydrogen released is important in containment analysis.

This paper discusses the various phenomena associated with channel behaviour and demonstrates how these are incorporated into safety analysis using the example of the assessment of a postulated loss of coolant/loss of emergency core cooling accident.

16.1 Introduction

Safety analysis must demonstrate that for the particular postulated accident being assessed, any resulting radiation dose to a member of the public, either an individual or a collective population, does not exceed the guidelines specified by the Atomic Energy Control Board. To determine this dose, fission product behaviour must be assessed from the time of its initial release from the fuel, at the onset of sheath failure, if any, to its release from containment and eventual airborne dispersion. In postulated severe accident conditions (i.e. failure of the main and backup PHT cooling systems), high temperature transient channel behaviour plays an important role in affecting the release from the fuel, since it greatly influences the thermal behaviour of the fuel bundles within the entire 6 m length of channel. Channel behaviour also plays an important role in determining the possible release of hydrogen into containment, which must then be assessed as part of containment analysis.

The core of a 600 MW(e) CANDU reactor consists of 380 individual fuel channels as shown in Figure 16.1. Each fuel channel is approximately 6 m long and contains 12 fuel bundles. The bundles are surrounded by a pressure tube and a calandria tube, with a gap containing insulating gas between them. The calandria tubes are surrounded by a low temperature heavy water moderator. This setup is illustrated in Figure 16.2.

Under postulated accident conditions such as those resulting from a loss of coolant and a coincident impairment of the emergency core cooling system, the heat generated in the fuel would be transferred mainly by thermal radiation to the pressure tube and to the calandria tube and then by boiling heat transfer to the moderator. Because radiation is the principal mode of heat transfer, high temperatures in the fuel and pressure tube result. At these elevated temperatures a chemical reaction between steam and the zircaloy, in the fuel sheaths and pressure tubes, occurs producing hydrogen and heat. The pressure tube deforms due to high temperature creep and contact with the calandria tube can occur (Figure 16.3). If the internal pressure within the channel is high, the principal deflection of the pressure tube is radially outwards and contact with the calandria tube occurs completely around the circumference (Figure 16.2). If the channel pressure is low, then the principal deflection is downward, and contact occurs in an eliptical patch on the bottom, as shown in Figure 16.5.

The initial contact between the hot pressure tube and the cold calandria tube would result in a sudden increase in the heat flux to the moderator. The magnitude of the peak would depend on the pressure tube temperature at contact and the contact conductance between the pressure and calandria tubes. The magnitude of the heat flux peak combined with the temperature of the water surrounding the calandria tube, determines the boiling regime on the calandria tube surface and thus the rate of heat removal. If nucleate boiling is predicted to occur, the stored energy of the pressure tube is quickly removed (Figure 16.6) and the fuel radiates to a low temperature pressure tube. If film boiling is the predicted mode of heat transfer (i.e. the sudden contact has resulted in the critical heat flux being exceeded) the stored energy of the pressure tube is not initially removed. Heat generated in the fuel radiates to a higher temperature pressure tube, until the calandria tube surface rewets and the situation is returned to the nucleate boiling condition as illustrated in Figure 16.7.

16.2 Pressure Tube Circumferential Strain Behaviour

The pressure tube material currently used in CANDU reactors is Zr-2.5% Nb. To model pressure tube deformation during a postulated high temperature transient condition, information regarding the creep rate of this material must be known. Although similar to the material currently used in fuel sheathing, Zr-4, to which substantial investigation at CRNL has been carried out, there are some significant differences which warrants specific investigation into the deformation behaviour of Zr-2.5% Nb. This experimental work is principally

carried out at Whiteshell Nuclear Research Establishment (Reference 16.1). The experimental program is divided into three areas. These are:

(1) Constant temperature and stress uniaxial tensile tests performed on specimens cut from pressure tube in both the longitudinal and transverse directions, as shown in Figure 16.8. These are used to arrive at basic creep-rate equations which can then be used to model pressure tube deformation.

(2) Investigation into the microstructural behaviour of Zr-2.5% Nb. This information factors into the creep rate equations mentioned in (1) above.

(3) Biaxial tests on short internally pressurized pressure tube sections (Figure 16.9), in order to verify the modelling of pressure tube behaviour using the information derived from (1) and (2), and to investigate the effect of non-uniform circumferential temperature distributions on pressure tube behaviour.

Based on the above mentioned work, a one-dimensional model called CONTACT (Reference 16.2) has been developed to predict the uniform circumferential strain behaviour of the pressure tube both prior to, and following contact with the calandria tube during high temperature transient conditions.

The deformation of the pressure tube prior to contact is calculated assuming that deformation is time-dependent (creep). The transverse creep rate of an internally pressurized tube is given by

$$\dot{\varepsilon}_t = A \exp\left(\frac{-Q}{RT}\right) \sigma_t^n$$

where $\dot{\varepsilon}$ is the transverse creep rate

A is the creep constant

Q is the creep activation energy

R is the ideal gas constant

T is the temperature

σ_t is the transverse stress

n is the stress exponent.

Substituting

$$\dot{\varepsilon}_t = \frac{1}{r}\frac{dr}{dt} \text{ and } \sigma_t = \frac{Pr}{w}$$

where r is the radius

t is time

P is the internal pressure

w is the wall thickness

and using the fact that the volume is constant, yields the following expression,

which can be integrated numerically to obtain the inner radius of the pressure tube at any time t:

$$r = r_o + \int_{t_o}^{t} A \exp\left(-\frac{Q}{RT}\right) r \left(\frac{Pr^2}{r_o w_o}\right)^n dt$$

where r_o is the original inner radius

w_o is the original wall thickness.

After contact, the pressure and calandria tubes creep at the same rate. Thus

$$A_c \exp\left(\frac{-Q_c}{RT_c}\right)\left(\frac{P_c r}{w_c}\right)^n = A_p \exp\left(\frac{-Q_p}{RT_p}\right)\left(\frac{(P-P_c)r}{w_p}\right)^n$$

where subscript c refers to the calandria tube, subscript p refers to the pressure tube, and r is the inner radius of the combined pressure/calandria tube.

Using the value of P_c determined from the above equation, the pressure-tube radius can be determined by numerically integrating

$$r \; r_c + \int_{t_o}^{t} A_p \exp\left(\frac{-Q_p}{RT_p}\right) r \left(\frac{(P-P_c)r^2}{r_o w_o}\right)^n dt$$

Predictions using CONTACT indicate that the temperature at which the pressure tube contacts its surrounding calandria tube is principally a function of the internal pressure and heat-up rate. Figure 16.10 illustrates the relationship between these variables. For any given constant pressure, the contact temperature generally increases with increasing linear pressure tube heat-up rate. For any given heat-up rate, a lower pressure results in higher contact temperature.

16.3 Channel Behaviour Following Pressure Tube/Calandria Tube Contact Resulting from Pressure Tube Circumferential Strain

The post contact behaviour of a channel can be predicted using the combined thermal/mechanical model CONTACT. The thermal model predicts the transient heat transfer along a radius through the pressure and calandria tubes. The heat conduction equation is solved using a one-dimensional finite-element routine. In order to solve for the pressure tube and calandria tube temperature the boundary conditions must be know. The boundary condition on the inside surface of the pressure tube is an incident heat flux, which is determined by the heat generated in the fuel due to the decay heat and the reaction between zirconium and steam.

The heat flux at the outside surface of the calandria tube is described by

$$q_o = h_b(T_{co}-T_B)$$

where q_o is the heat flux to the moderator

h_b is the pool-boiling heat-transfer coefficient

T_{co} is the outside temperature of the calandria tube

T_B is the bulk moderator temperature.

The heat-transfer coefficient, h_b, depends on the type of boiling that occurs with the given subcooling, the saturation temperature, the outside surface temperature of the calandria tube, and the heat flux. In the model, h_b is defined for four regimes as shown in Figure 16.11 (Reference 16.3, 16.4): subcooled, nucleate boiling, transition boiling, and film boiling. The equations were based on experiments by Thibault (Reference 16.5), Rohsenow (Reference 16.6) Bradfield (Reference 16.7) and Dhir and Purchit (Reference 16.8), using large diameter horizontal cylinders.

At the interface between the pressure and calandria tubes, the contact conductance determines the rate at which the heat stored in the pressure tube is transferred to the moderator immediately after contact; thus, it also affects the pool-boiling regime. The contact conductance, h_c, is described by the following relationship:

$$q_c = h_c\,(T_{po} - T_{ci})$$

where q_c is the heat flux between the tubes

h_c is the contact conductance

T_{po} is the temperature of the outer surface of the pressure tube

T_{ci} is the temperature of the inner surface of the calandria tube.

A great deal of information has been obtained through the combined use of the above mentioned model and experiments designed specifically to investigate this behaviour. These experiments, performed at WNRE (References 16.2, 16.3 and 16.4) investigated the thermal and mechanical behaviour when a pressure tube creeps circumferentially into contact with its calandria tube. These 'CONTACT BOILING' experiments were performed by heating an internally pressurized length of pressure tube so that it expands radially into contact with its surrounding section of calandria tube which is immersed in a tank of water. The ensuring boiling process on the surface of the calandria tube is then observed. Figures 16.12 and 16.13 show the experimental setup and what can be observed through the viewing port during a test.

Information generated through this investigation has demonstrated that the heat removal from the pressure tube is controlled by the type of boiling which occurs on the surface of the calandria tube. The factors which affect which type of boiling takes place are:

(1) The temperature at which the pressure tube contacts the calandria tube (briefly discussed in Section 16.3). This is important as it is the driving force for the peak in the transient heat flux which will be experienced at the outside surface of the calandria tube, almost immediately upon contact.

(2) The contact conductance between the pressure tube and calandria tube (a function of the contact pressure, surface hardness and roughness) since it offers a resistance to the heat flux experienced at the outer surface of the calandria tube.

(3) The subcooling at the surface of the calandria tube (difference between the local saturation temperature and the local water temperature) as this determines the value of the critical heat flux.

The relationship between these variables and the type of boiling which occurs on the calandria tube surface is illustrated in Figure 16.14. Each experiment represents a point on the graph, with the pressure tube temperature at contact as the abscissa and the subcooling of the water pool surrounding the calandria tube as the ordinate. The type of boiling on the calandria-tube surface during the experiment is denoted by the symbols. Also shown are lines for different assumed contact conductances, showing where the peak heat flux to the moderator at contact, as predicted by CONTACT, equals the critical heat flux. Film boiling occurs when the peak heat flux exceeds or equals the critical heat flux; thus, film boiling is predicted for points plotted on the graph above the line if the assumed contact conductance is correct.

In each experiment, the internal pressure was held constant at a value ranging from 0.5 to 4.0 MPa. Table 16.1 indicates the pressure at which each test was performed. The results plotted in Figure 16.14 indicate that, for all of the experiments with an internal pressure of 1 MPa or greater, the maximum local contact conductance was 11 kW/(m^2.^oC) since the type of boiling on the surface was correctly predicted using this value. The patchiness of the film boiling indicates that the contact conductance was less than this maximum for most areas around the circumference. In the experiments performed at pressures of 0.7 and 0.5 MPa, the maximum contact conductance was less than 11 kW/(m^2.^oC), since film boiling would be predicted, and it did not occur. The use of this method to determine the contact conductance assumes that the incident heat flux, determined from the known heater power, and the heat-transfer coefficient at the surface of the calandria tube used in this model, are known.

In nine of the experiments, film boiling occurred in patches that did not completely cover the area of contact. This behaviour is related to the variation of contact time, temperature, and pressure at a given axial location. The variation of these parameters causes the contact conductance to vary around the circumference.

The patches of film boiling rewet, even when the average incident heat flux is higher than the minimum heat flux required to maintain film boiling. The rewetting is caused by the axial and circumferential conduction of heat through the pressure and calandria tubes from areas of film boiling to areas of nucleate boiling (Figure 16.15).

From the safety analysis point of view, the occurrence of film boiling is important in that it could potentially jeopardize channel integrity. Since the film boiling heat transfer coefficient is significantly lower than that for nucleate boiling (Figure 16.11), the calandria tube experiences a marked increase in temperature and hence reduced strength. Under severe conditions such as high internal pressure, high incident heat flux onto the surface of the pressure tube, and low subcooling on the calandria tube surface, the channel may strain to the point of rupture. An experiment designed to investigate this behaviour demonstrated that the conditions must be considerably more severe than those originally believed, to result in rupture of the calandria tube. This was due to the increased heat transfer to the water resulting from the increased calandria tube surface area, as the tube expanded (Figures 16.16 and 16.17).

16.4 Pressure Tube Sag

Under high temperature but low pressure conditions, the pressure tube will reach the point where it can no longer support its own weight and that of the fuel. It then begins to sag and contact the calandria tube resulting in an elliptically shaped contact area at the bottom of the channel. While the pressure tube temperature in the contact area (see Figure 16.4) is reduced by the process described in the previous section, the top of the pressure tube can continue to rise in temperature. If the channel remains somewhat pressurized, the pressure tube could deform radially outwards, contacting the calandria tube completely around the circumference and its behaviour thereafter would be similar to that discussed in the previous section.

The sag behaviour of a fuel channel under high temperature conditions is modelled by the computer program CREEPSAG (Reference 16.9). CREEPSAG calculates the axial, transverse and bending creep strains of a pressure tube/calandria tube system as a function of time taking into account the elastic support forces at the garter springs and the ends of the channel. A series of experiments were performed to verify the predictions of the program and to investigate the overall behaviour under these conditions.

The latest series of experiments which have been performed to investigate sag behaviour is the large scale pressurized fuel channel sag experiments. In these tests, the deformation and resulting contact behaviour of a 3 m long pressure tube/calandria tube assembly, as shown in Figure 16.18 is investigated. The method by which the pressure tube is heated, shown in Figure 16.19 produces a heat flux incident onto the surface of the pressure tube which is equivalent to that predicted under decay power conditions. It also simulates the weight of the fuel. By pressurizing the fuel channel the combined mode of pressure tube deformation is investigated.

Results from these experiments have shown that:

(1) In the case of sag contact under non-pressurized conditions, contact between the pressure tube and calandria tube takes place in a small elliptical patch on the bottom of the channel.

(2) Although garter springs increase the contact temperature over the case in which no mid-length pressure tube support was available, the distance between the garter springs is not too important since local plastic deformation of the pressure tube, around each garter spring, tends to result in contact in the 800-850^{o}C temperature region.

(3) The contact conductance between the pressure tube and calandria tube is less than that for the case of diametral strain at higher pressure, since the bending moments in the pressure tube cause a reduction in contact pressure.

16.5 The Application of High Temperature Transient Channel Behaviour to the Assessment of a Postulated Loss of Coolant/Loss of Emergency Core Cooling Accident in a CANDU Reactor

The methodology currently used by the Engineering Company of AECL to assess postulated LOC/LOECC accidents is to divide the analysis into two consecutive segments as illustrated in Figure 16.20. The first of these is referred to as the 'front end assessment'. It uses techniques developed from the classical loss of coolant accident analyses. Here thermohydraulics during the transient is predicted using a network model incorporating the features found in a CANDU primary heat transport system (Reference 16-10). The depressurization transient predicted by this type of model for a certain break in the reactor inlet header is shown in Figure 16.21. These and other thermohydraulic conditions are then used to determine the channel behaviour using HOTSPOT (Reference 16.11) and CONTACT-1. HOTSPOT models a 37 element fuel bundle surrounded by its pressure tube, calandria tube and moderator. It is used to determine the temperature of the fuel, sheath and pressure tube, given the thermohydraulic information of coolant temperature and sheath to coolant heat transfer coefficient. HOTSPOT models thermal radiation between

each element and to the pressure tube. It also takes into account the exothermic reaction which takes place between the zircaloy and the steam. HOTSPOT also incorporates the CONTACT model so uniform circumferential strain and the resulting behaviour can be assessed.

After some point in time, the methodology calls for a transfer into a classical LOC/LOECC type of approach. Here, where uncertainty in the flowrate of steam down the channel exists, a different approach is taken. Starting from initial conditions determined from the front end assessment, the late core assessment treats the flow of steam entering the channel as a parameter and assesses its effect on fission product release and hydrogen generation. This assessment is carried out using the computer program CHAN-II (Reference 16.12, 16.13).

CHAN-II models a single channel dividing it up into 12 segments as shown in Figure 16.22. These segments coincide with the 12 half metre long fuel bundles. In each axial segment, the fuel elements, pressure tube and calandria tube are modelled by a system of annular rings as shown in Figure 16.23. Steam at a specified temperature and rate enters the channel at one end, while a steam/hydrogen mixture exits at the other after a heat and mass balance has been performed on each segment. This is performed by solving a set of time dependent differential equations derived from a lumped parameter analysis of the heat generated in the fuel channel, the convective axial heat transfer by flowing steam and hydrogen and the radial heat transfer to the moderator by radiation and conduction.

To assess the effect of sag contact, the temperatures can be determined in two regions, the contact and non-contact zones as illustrated in Figure 16.23. Results using this model have shown that while the pressure tube and fuel temperatures in the contact zone decrease following contact, those in the non-contact region continue to heat-up and reach significantly higher levels.

CHAN-II analysis has demonstrated that a trade-off exists between the convective cooling supplied by the steam flow and the heat generated by the exothermic reaction between the zircaloy in the fuel sheaths and pressure tube with the oxygen supplied by the steam. At low flow rates, although there is little convective heat transfer, there is not enough steam to support the oxidation process. At very high flow rates, the heat generated in the fuel is removed by enhanced convective cooling and the temperatures remain below that at which metal water reaction becomes significant (approximately 1000^{o}C). Over a small range of predicted flows, fuel temperatures and hence hydrogen production and fission product release reach a maximum. This behaviour is illustrated in Figure 16.24 which plots hydrogen production as a function of constant steam flow rate entering the channel. By superimposing the results for separate channels, the overall behaviour of the core can be assessed.

In the assessment of the overall response of the core to a postulated LOC/LOECC accident, information from CHAN-II is used to:

(1) Determine fission product release which is later used in arriving at the dose estimate.

(2) Determine the heat load to the moderator as a result of the channels which undergo contact. This information is then used in determining the moderator transient temperature which in turn is required to assess channel integrity.

(3) Determine the hydrogen source term originating from the metal/water reaction ($Zr + H_2O \rightarrow ZrO_2 + 2H_2 + E$) which then is used in containment calculations to investigate the behaviour of hydrogen within the containment (Figure 16.25).

Figure 16.26 is a representation of a characteristic temperature versus time response of a fuel channel segment of a high power channel (7.4 MW) with a 'critical steam flowrate'. The axial temperature profile when the maximum temperature occurs is shown in Figure 16.27. As can be observed from these graphs, the temperature transients experienced by the fuel is very severe, but still not high enough to reach the 2840°C melting temperature of the UO_2. Channels operating at much lower powers do not experience transients of this severity, as shown in Figure 16.28. An overall behaviour of the core can be investigated by superimposing the results for various channel powers and steam flow rates.

To assess channel integrity, the models described in the preceeding sections were employed as follows:

The temperature at which the pressure tube contacted the calandria tube was determined by the type of deformation. Up to 850°C, the circumferential strain was modelled using the FIREBIRD-III predicted depressurization transient and the pressure tube temperature history predicted by HOTSPOT and CHAN-II. If contact was not predicted prior to 850°C, the pressure tube was assumed to sag into contact with the calandria tube, as discussed in Section 16.5.

The contact conductance between the contacting pressure tube and calandria tube depends on the deformation mode. If circumferential strain to contact is predicted, the contact conductance is assumed to be 11 kW/m^2°C, as discussed in Section 16.4. If pressure tube sag is the assumed deformation mode, a value of 6.5 kW/m^2°C is used for contact conductance.

The last remaining parameter which could determine the boiling regime on the calandria tube surface when contact occurs, is the moderator subcooling. These values were determined by combining information from the predicted steady-state multi-dimensional moderator temperature distribution and the ensuing moderator temperature transient resulting from the drop in neutron-gamma heat load and the increase in the heat load from calandria tubes resulting from contact with their pressure tubes. The steady-state moderator temperature distribution was determined by techniques described in Reference 16.14. Predictions using this model demonstrate the possible existence of two different types of flow

patterns as shown in Figure 16.29. These are the jet momentum dominated and the bouyancy dominated flow patterns. Preliminary results from experiments have confirmed this as well as shown the existance of a combined momentum/bouyancy pattern.

The temperature transient experienced by the moderator following the postulated break is determined by the heat load transient it experiences. The major contributing source of moderator heating during normal operations conditions is due to neutron-gamma heating. As shown in Figure 16.30 following the initial break there is a small rise due to the power pulse associated with the coolant void, but then it rapidly drops off to an extremely low level following reactor trip. The heat load to the moderator from the calandria tubes is determined by CHAN-II in conjunction with HOTSPOT and CONTACT. A typical heat load to the moderator resulting from contacting channels in the broken loop, for assumed constant steam flowrate of 10 s/s, is shown in Figure 16.31. The front end spikes results from sections of groups of channels contacting due to circumferential strain. The longer term peak, which is much smaller than the normal operating heat load and hence the reason why the moderator temperature decreases during the transient, is a result of sag contact and the ultimate transfer of heat generated within the channels of the broken loop. The automatic isolation of the loops following the loss-of-coolant signal limits the loss-ofcoolant accident to only one of the loops.

Combining the abovementioned information, current predictions indicate that nucleate boiling is the expected mode of heat transfer from the calandria tube surface following contact with the pressure tube. From this, and information presented in Section 16.4, it can be concluded that channel integrity is maintained even under these extremely severe hypothetical conditions.

16.6 Conclusion

The investigation of high temperature transient channel behaviour for CANDU reactors demonstrates the effectiveness of the moderator to act as a supplementary heat sink in order to prevent the melting of fuel and to preserve the integrity of the basic channel geometry. Because of this inherent safety feature, the probability of a core meltdown under even the most severe postulated accidents is negligible.

16.7 References

(16.1) R.S.W. Shewfelt and C.K. Chow, "Deformation of Zr-2.5% Nb Pressure from 400-1200°C", Paper Presented at the 21st Annual Conference of Metallurgists, Toronto, 1982.

(16.2) G.E. Gillespie, R.G. Moyer and P.D. Thompson, "Moderator Boiling on the External Surface of a Calandria Tube in a CANDU Reactor During a Loss of Coolant Accident", AECL-7664, Presented at the ANS Conference, Chicago, 1982 August.

(16.3) G.E. Gillespie, G. Moyer and R.S.W. Shewfelt, "Experiments to Investigate Moderator Boiling When a Pressure Tube Contacts its Calandria Tube", WNRE-401, 1980 August.

(16.4) G.E. Gillespie, "An Experimental Investigation of Heat Transfer from a Reactor Fuel Channel to Surrounding Water", CNS Conference, Ottawa, 1981 June.

(16.5) J. Thibault, "Boiling Heat Transfer Around a Horizontal Cylinder and in Tube Bundles", Ph.D. Thesis, McMaster University, Hamilton, Ontario, 1978.

(16.6) W.M. Rohsenow, ed., Developments in Heat Transfer, The MIT Press, Cambridge, Massachusetts, (1964) p. 216.

(16.7) W.S. Bardfield, "On the Effect of Subcooling on Wall Superheat in Pool Boiling", Journal of Heat Transfer 89, 269 (1967).

(16.8) V.K. Dhir and G.P. Purohit, "Subcooled Film-Boiling Heat Transfer from Spheres", Nuclear Engineering and Design 47, 49 (1978).

(16.9) R.S.W. Shewfelt and J.D. Bean, "Users Manual for CREEPSAG: A Computer Program for Analyzing the Creep Deformation of Fuel Channels", WNRE-338, January 1978.

(16.10) M.R. Lin et al, "FIREBIRD-III Program Description", TDAI-166, Volume 1, 1979 September.

(16.11) R.E. Pauls, "HOTSPOT: A Computer Code for Predicting the Fuel Bundle Temperature Distribution History Following a LOCA", Report GP-75-064, July 1975.

(16.12) V.Q. Tang and D.G. Vandenberghe, "CHAN-II: A Computer Program Predicting Fuel Channel Thermal Behaviour in a Typical CANDU-PHW Reactor Core Following a Loss of Coolant Accident", WNRE-494, 1981 July.

(16.13) G.E. Gillespie et al, "Thermal Behaviour of a CANDU-PHW Reactor Fuel Channel Containing Wearly Stagnant Steam", Presented at the ANS Conference, Chicago, August 1982.

(16.14) L.N. Carlucci, "Numerical Simulation of Moderator Flow and Temperature Distributions in a CANDU Reactor Vessel", Presented at the International Symposium on Refined Modelling of Flows, Paris, September 1982.

TABLE 16.1

SUMMARY OF CONDITIONS AND RESULTS OF ALL CONTACT BOILING EXPERIMENTS

TEST NUMBER	INTERNAL PRESSURE (MPa)	WATER POOL SUBCOOLING (^{o}C)	APPROXIMATE* PRESSURE TUBE CONTACT TEMPERATURE (^{o}C)	TYPE OF BOILING ON CALANDRIA TUBE SURFACE AND TIME TO QUENCH (s)	
POWER SHUT OFF AT CONTACT					
1	4.	32	Commissioning test	-	-
2	4.	32	712 - 748	-	-
3	4.	14	706 - 745	NB	-
4	1.	25	823 - 835	FB	30
5	1.	32	826 - 844	FB	16
6	2.5	22	643 - 732	NB	-
7	4.	18	674 - 733	NB	-
8	2.5	22	734 - 808	FB	6
9	2.5	22	765 - 796	FB	10
POWER MAINTAINED AFTER CONTACT					
10	1.	20	905	FB	20
11	4.	14	684 - 741	FB	10
12	0.3	15	820	FB	40
13	1.	15	1000	FB	470
14	1.		Heater failure		
15	0.5	28	Heater failure		
16	0.5	28	950 - 1050	NB	
17	1.	14	850 (garter springs)	FB	100
18	4.	14	740 (garter springs)	FB	
19	1.1	28	826	NB	-
20	0.75	27	900	NB	-
21	2.	0	800	FB	-

* Is a function of position around tube

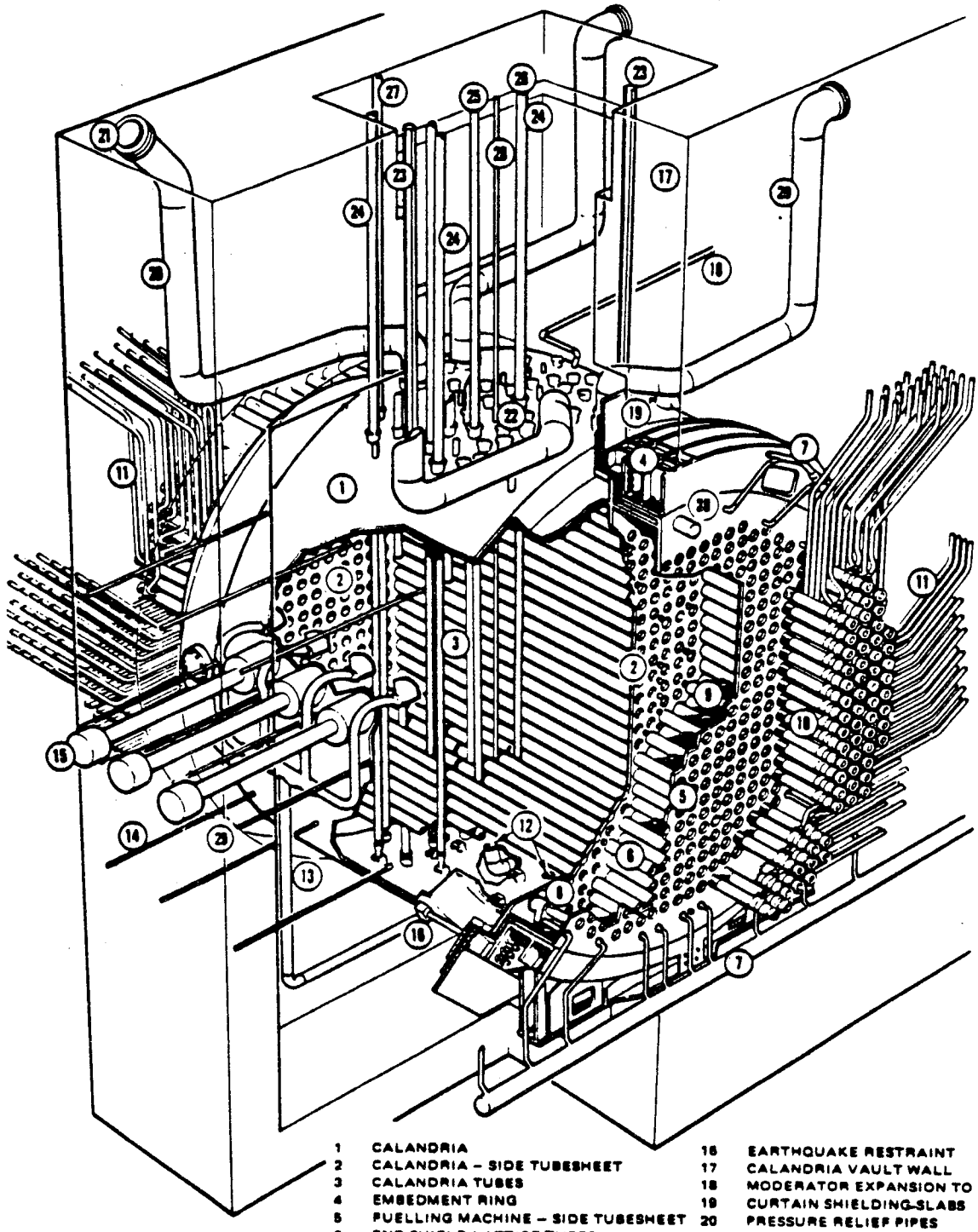

1	CALANDRIA	16	EARTHQUAKE RESTRAINT
2	CALANDRIA – SIDE TUBESHEET	17	CALANDRIA VAULT WALL
3	CALANDRIA TUBES	18	MODERATOR EXPANSION TO HEAD TANK
4	EMBEDMENT RING	19	CURTAIN SHIELDING SLABS
5	FUELLING MACHINE – SIDE TUBESHEET	20	PRESSURE RELIEF PIPES
6	END SHIELD LATTICE TUBES	21	RUPTURE DISC
7	END SHIELD COOLING PIPES	22	REACTIVITY CONTROL UNIT NOZZLES
8	INLET-OUTLET STRAINER	23	VIEWING PORT
9	STEEL BALL SHIELDING	24	SHUTOFF UNIT
10	END FITTINGS	25	ADJUSTER UNIT
11	FEEDER PIPES	26	CONTROL ABSORBER UNIT
12	MODERATOR OUTLET	27	ZONE CONTROL UNIT
13	MODERATOR INLET	28	VERTICAL FLUX DETECTOR UNIT
14	HORIZONTAL FLUX DETECTOR UNIT	29	LIQUID INJECTION SHUTDOWN NOZZLE
15	ION CHAMBER	30	BALL FILLING PIPE

REACTOR ASSEMBLY

FIGURE 16.1

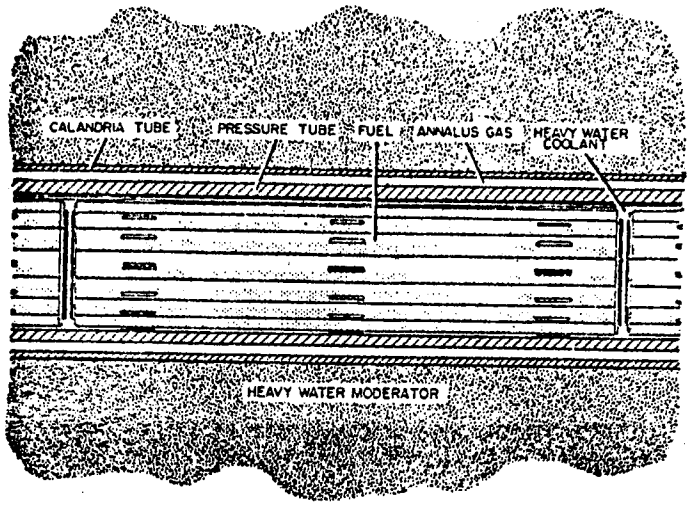

FUEL CHANNEL ARRANGEMENT

FIGURE 16.2

BACKGROUND

FAILURE OF ECC ➧ **LITTLE OR NO CONVECTIVE FUEL COOLING AFTER SHORT PERIOD OF TIME**

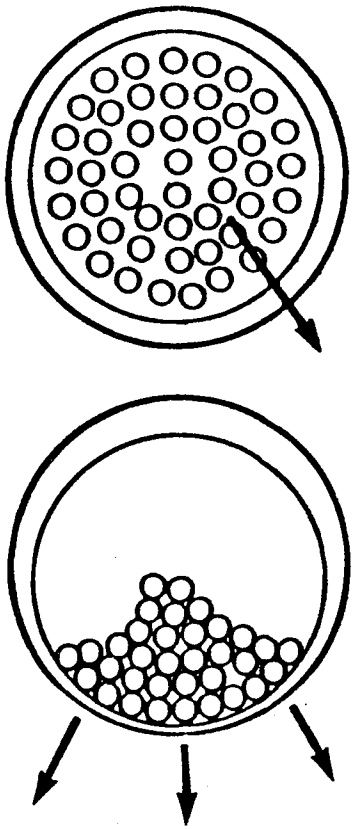

- Radiation to PT & CT
  Therefore $T_{fuel} + T_{PT}$ increases
- Boiling heat transfer to moderator
- MWR on fuel + PT ⟶ H_2
  ⟶ Heat
- Pressure tube deforms
- PT/CT contact occurs causing spike in heat flux

CT DRYOUT
?

NO
- Good heat path from fuel to moderator

YES
- Impaired heat removal
- Channel integrity in question

FIGURE 16.3

PRESSURE TUBE DIAMETRAL STRAIN

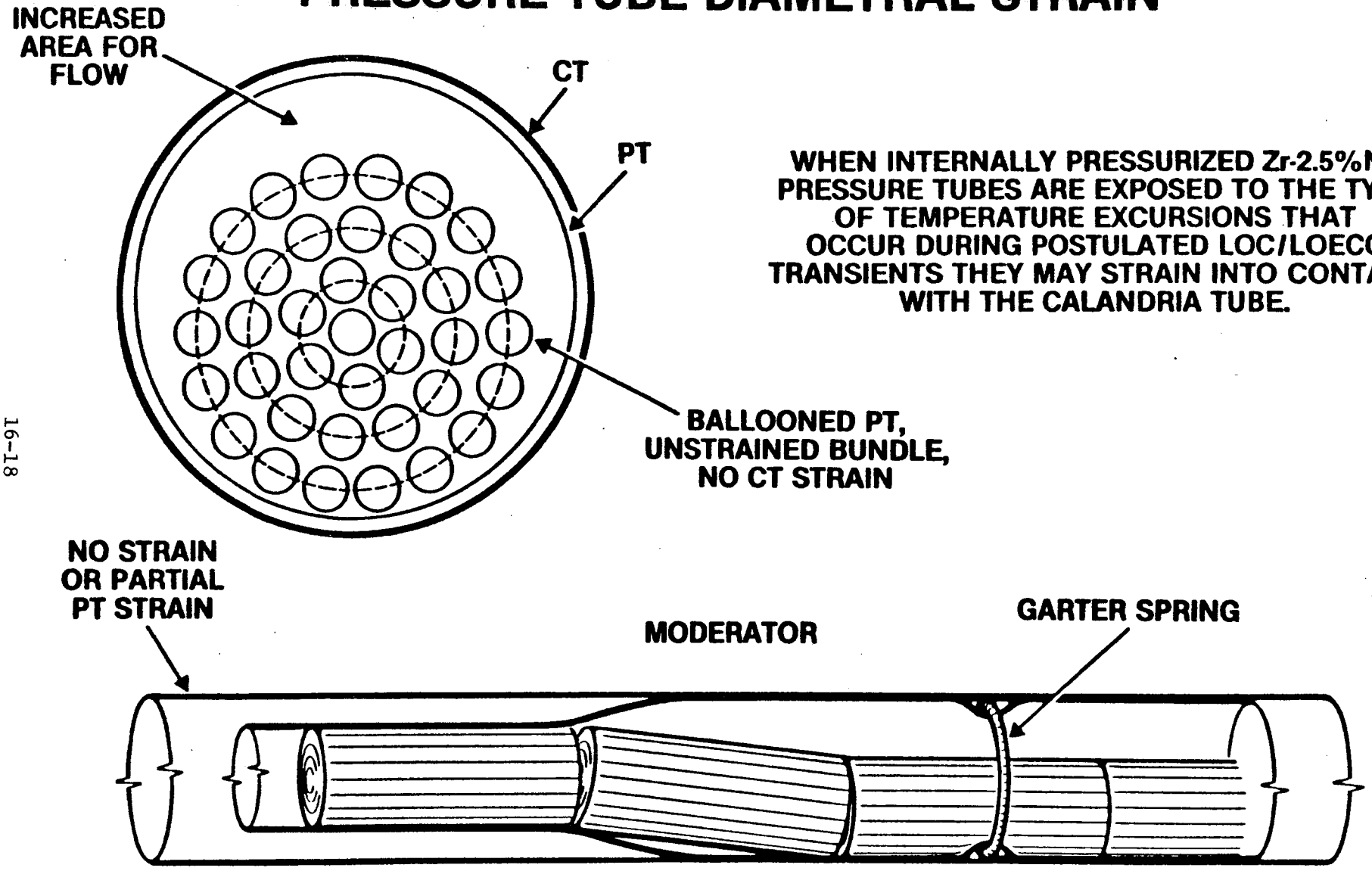

WHEN INTERNALLY PRESSURIZED Zr-2.5%Nb PRESSURE TUBES ARE EXPOSED TO THE TYPE OF TEMPERATURE EXCURSIONS THAT OCCUR DURING POSTULATED LOC/LOECC TRANSIENTS THEY MAY STRAIN INTO CONTACT WITH THE CALANDRIA TUBE.

FIGURE 16.4

PRESSURE TUBE SAG

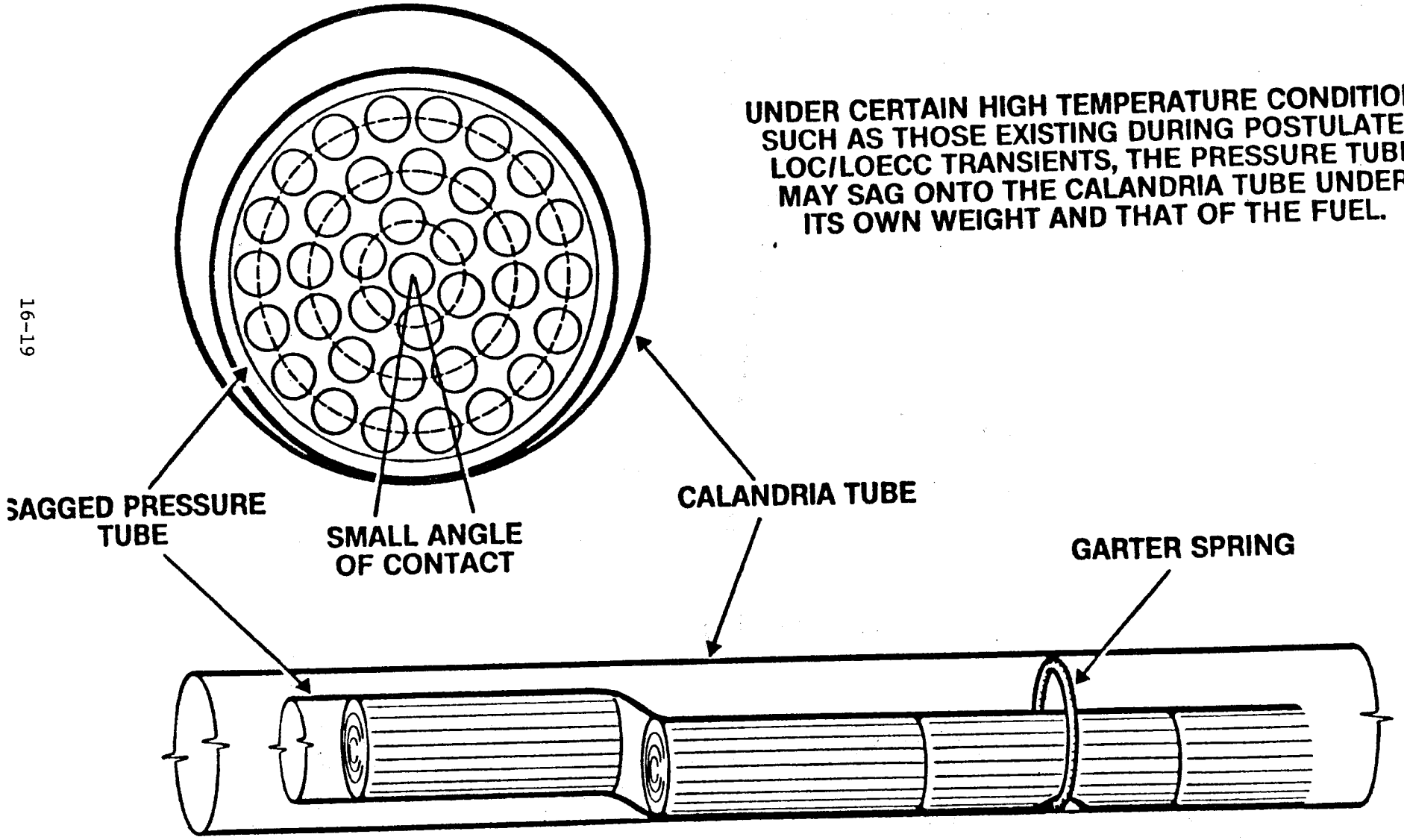

Figure 16.5 - Diagram of Channel in the Case of Pressure Tube Sag

THERMAL RESPONSE FOR CASE OF NO CALANDRIA TUBE DRYOUT

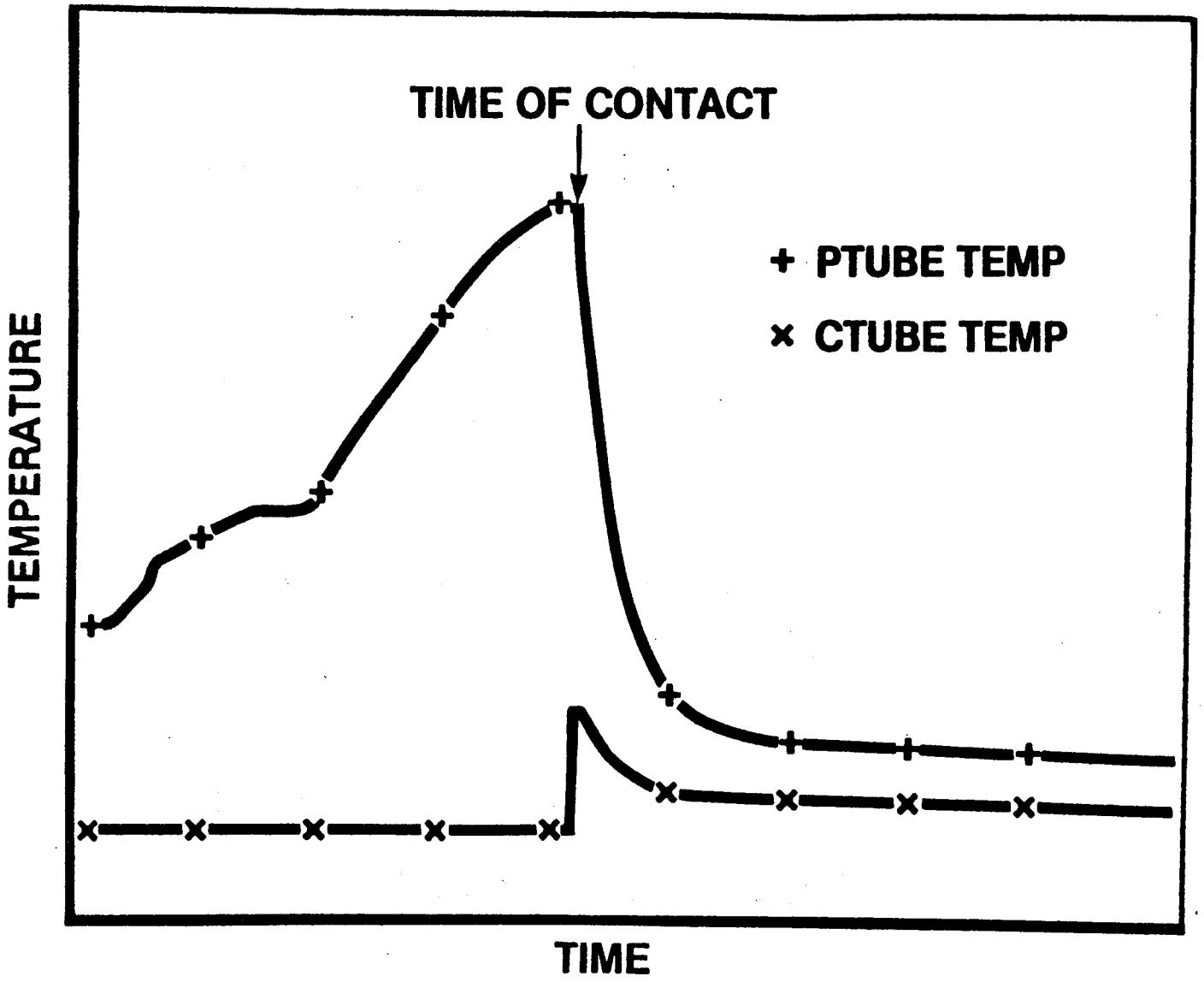

FIGURE 16.6

REPRESENTATIONAL PLOT OF THERMAL RESPONSE OF CHANNEL EXPERIENCING FILM BOILING

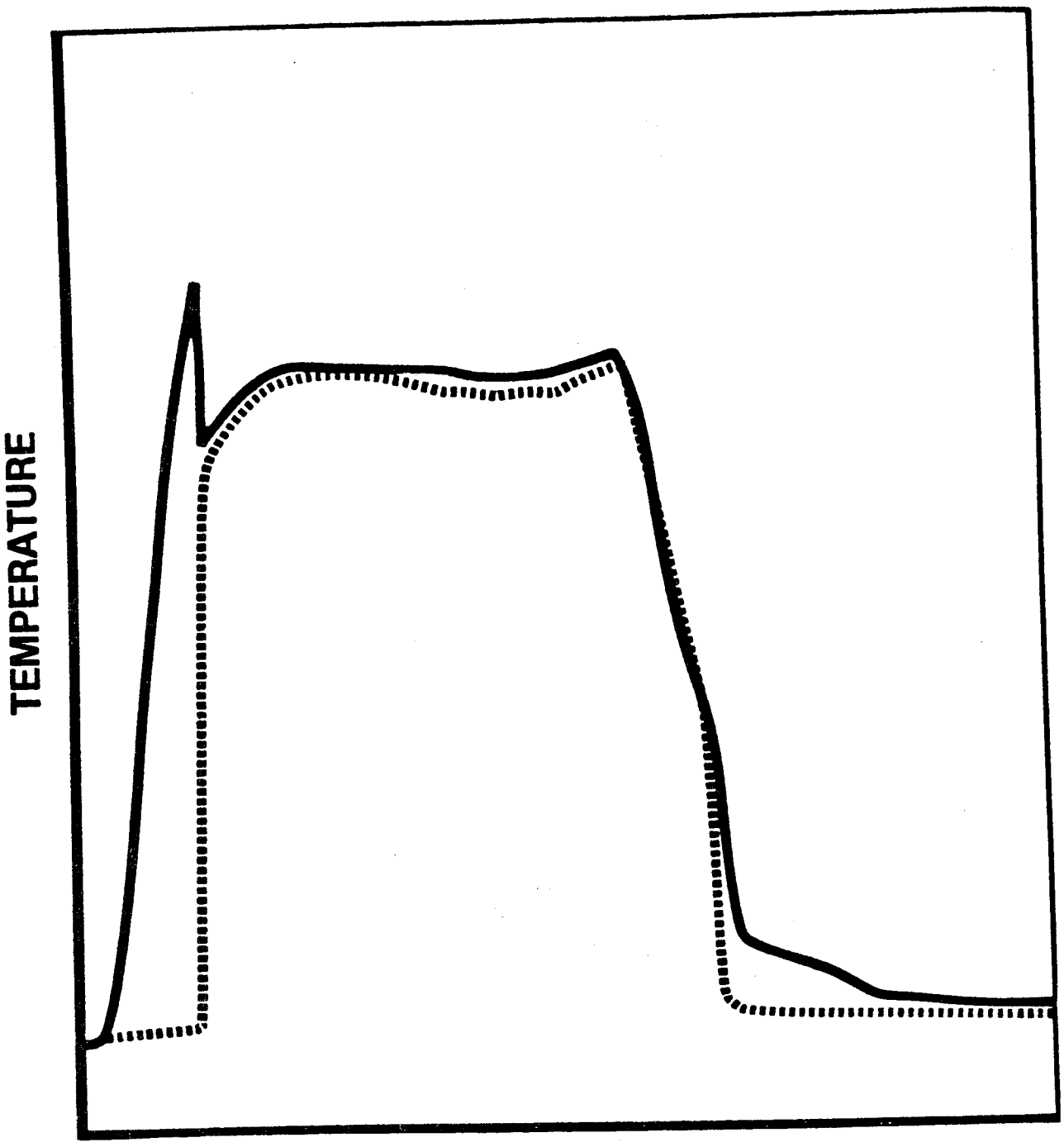

FIGURE 16.7

UNIAXIAL CREEP SPECIMENS

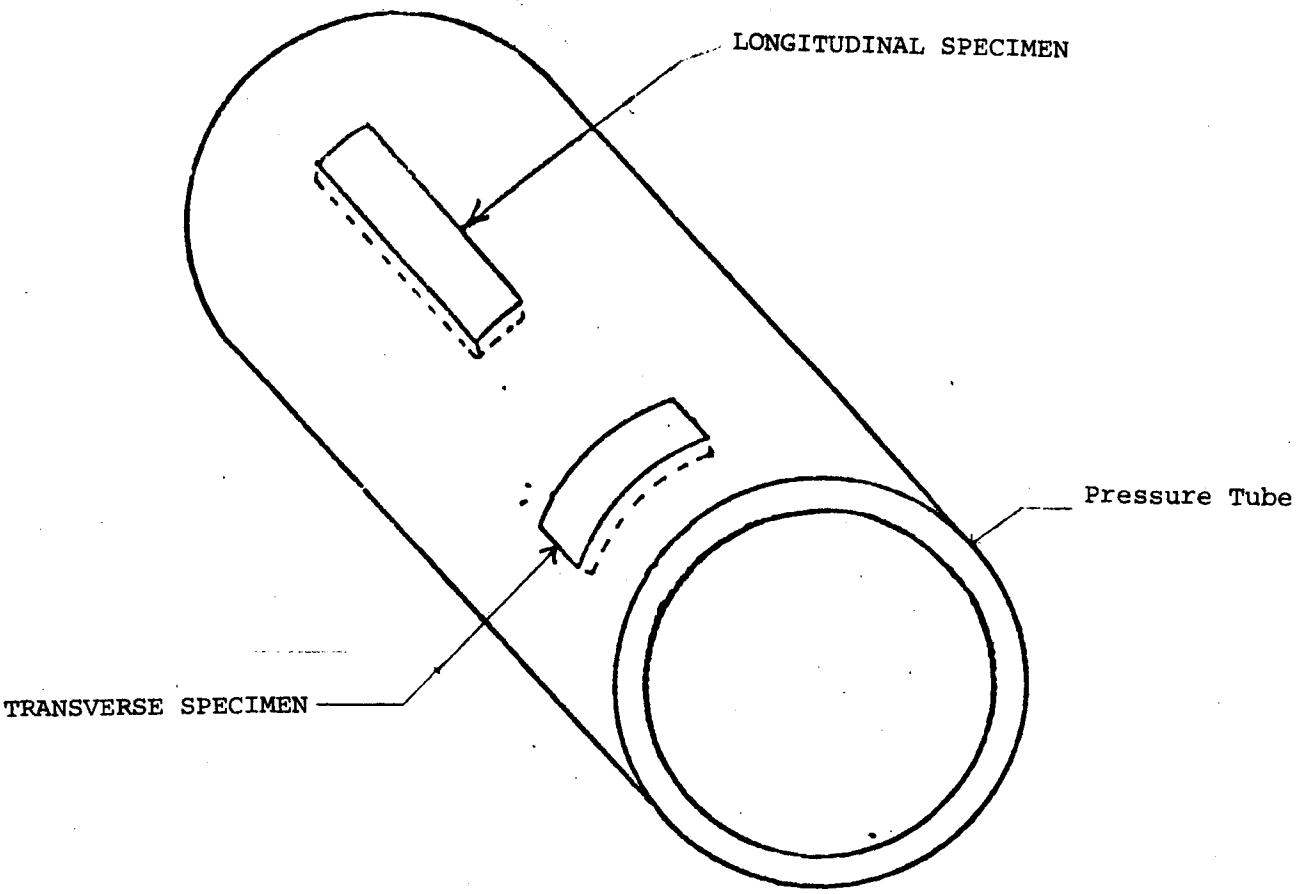

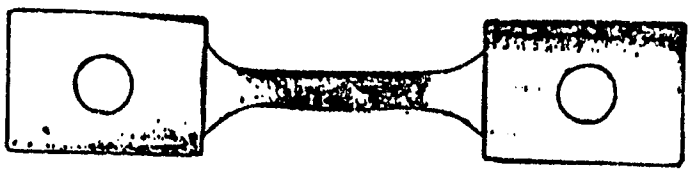

FIGURE 16.8 Actual size of specimen

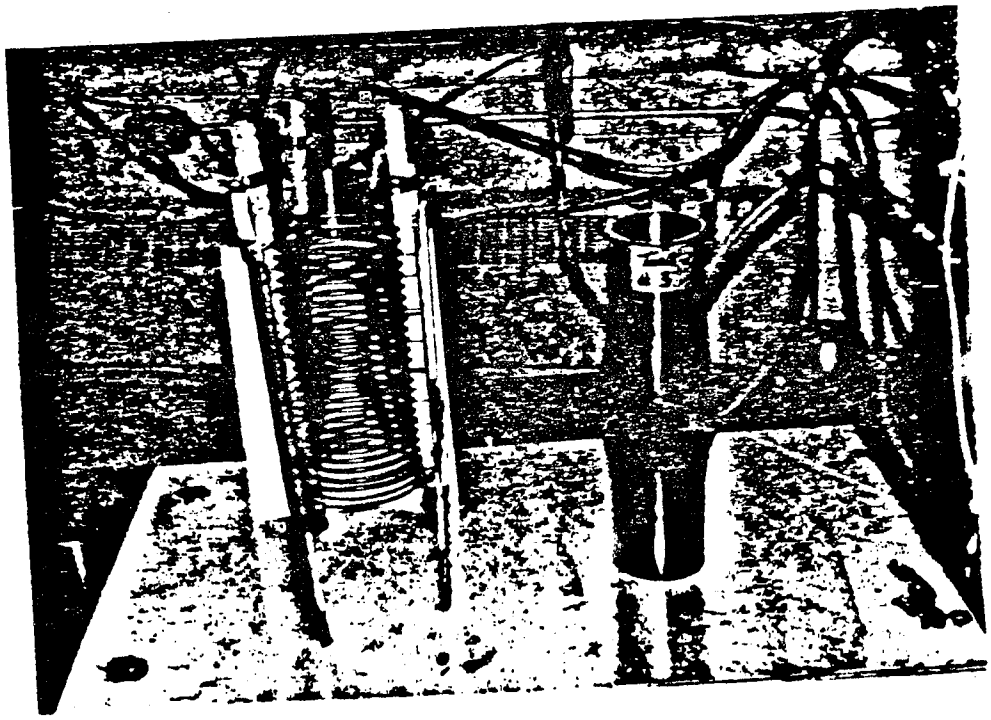

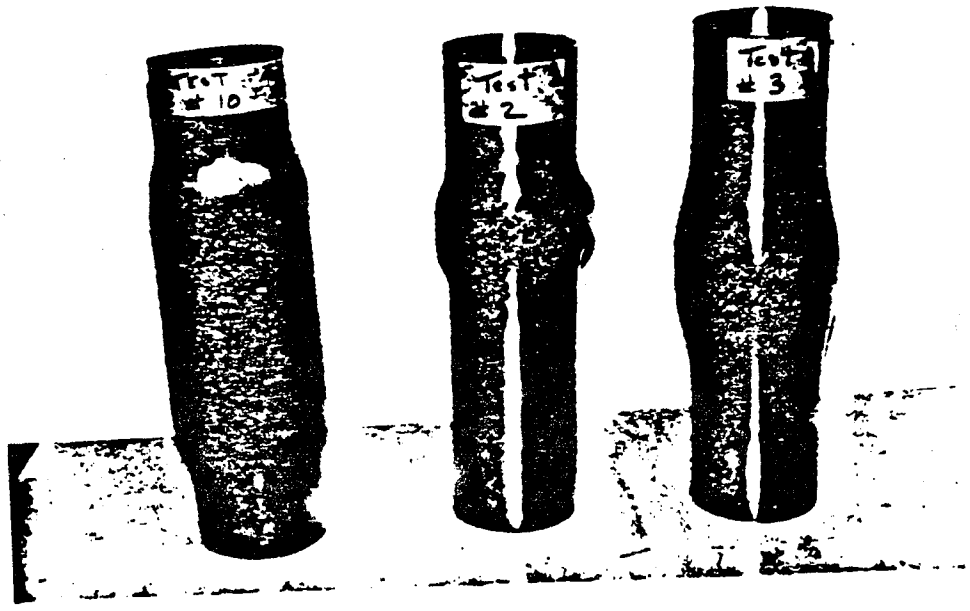

FIGURE 16.9

INDUCTION HEATER USED FOR BIAXIAL TESTS WITH STRAINED SPECIMENS

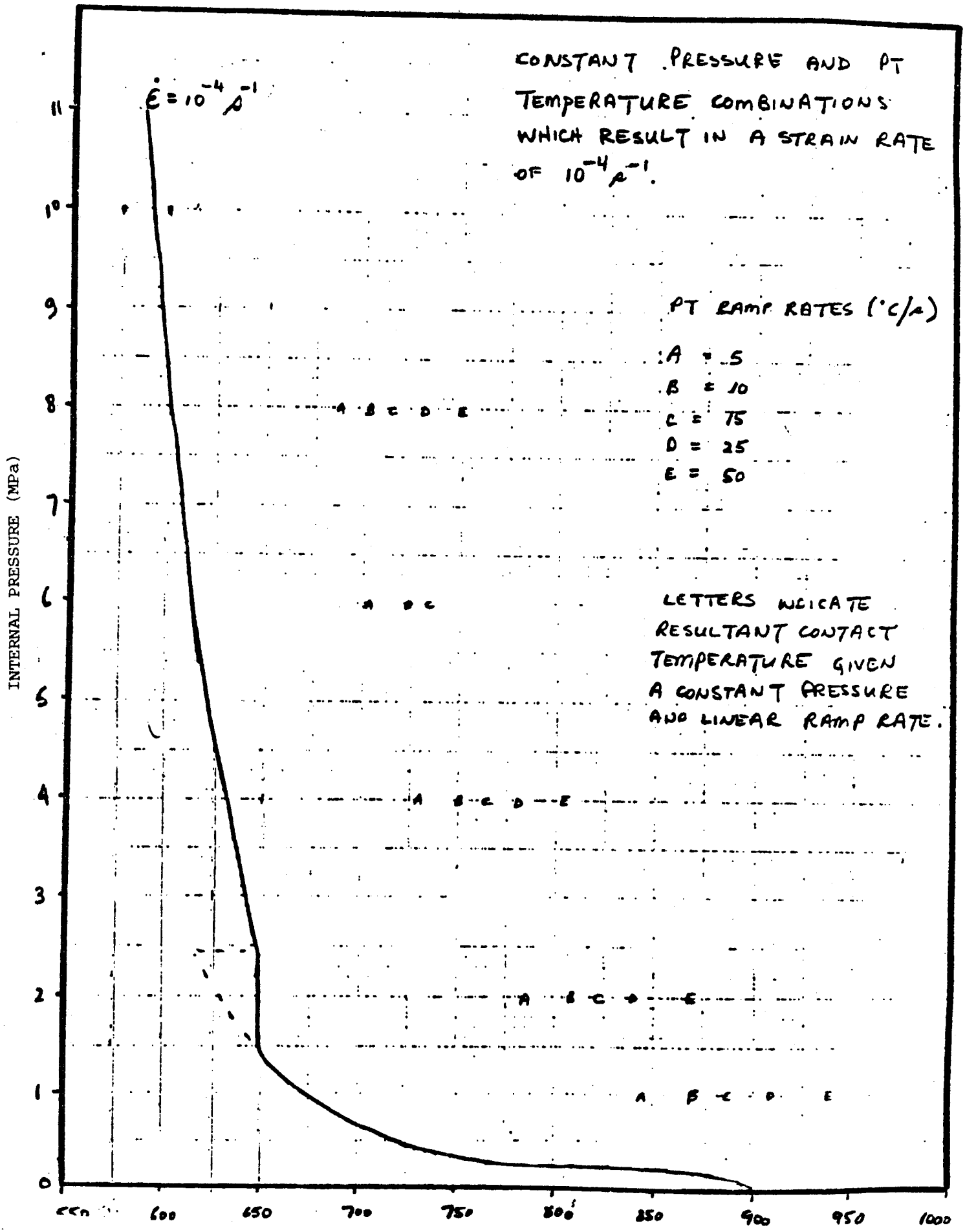

FIGURE 16.10 PRESSURE TUBE TEMPERATURE (oC)

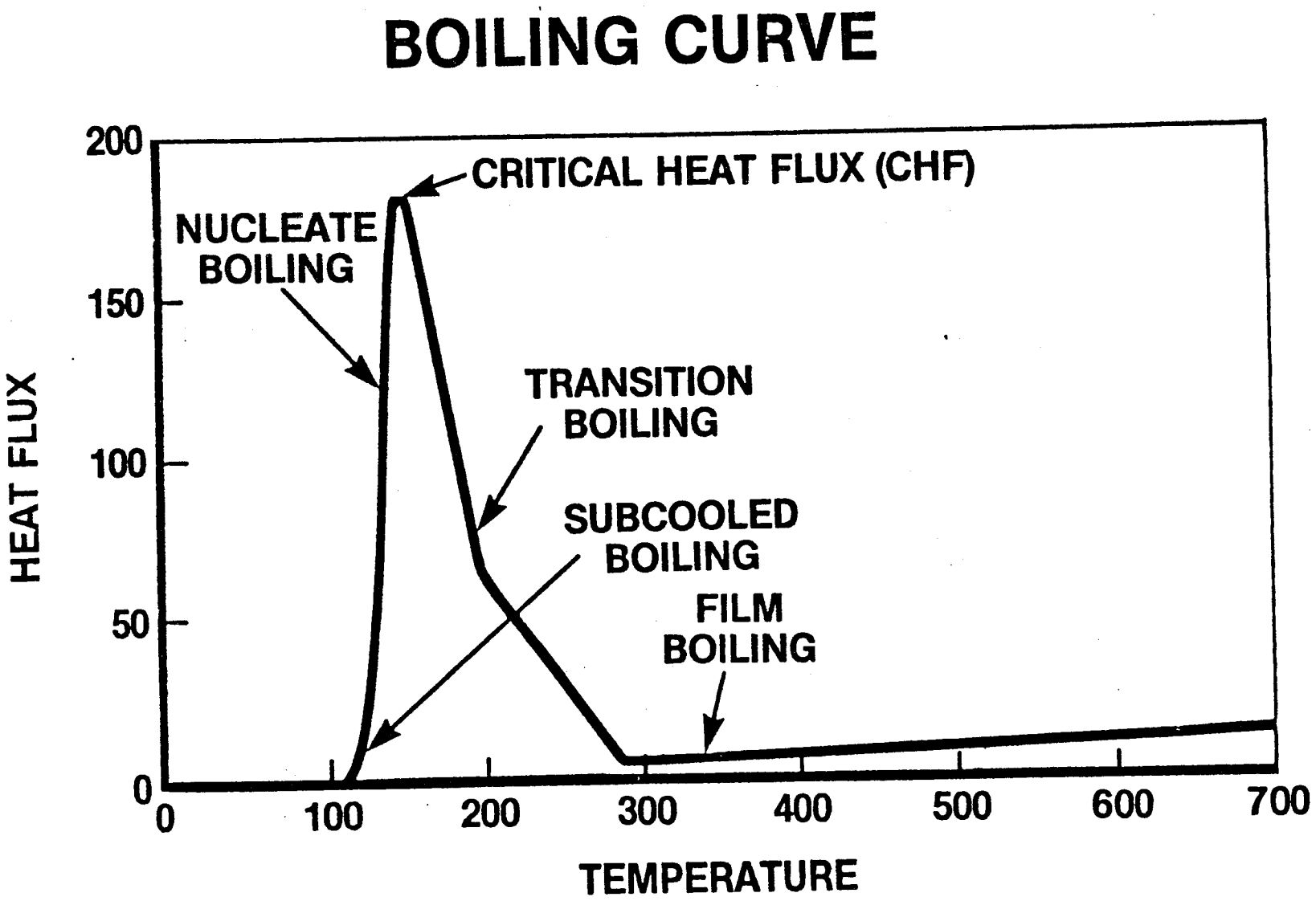
BOILING CURVE
200
150
100
50
0
HEAT FLUX
CRITICAL HEAT FLUX (CHF)
NUCLEATE BOILING
TRANSITION BOILING
SUBCOOLED BOILING
FILM BOILING
0
100
200
300
400
500
600
700
TEMPERATURE

FIGURE 16.11

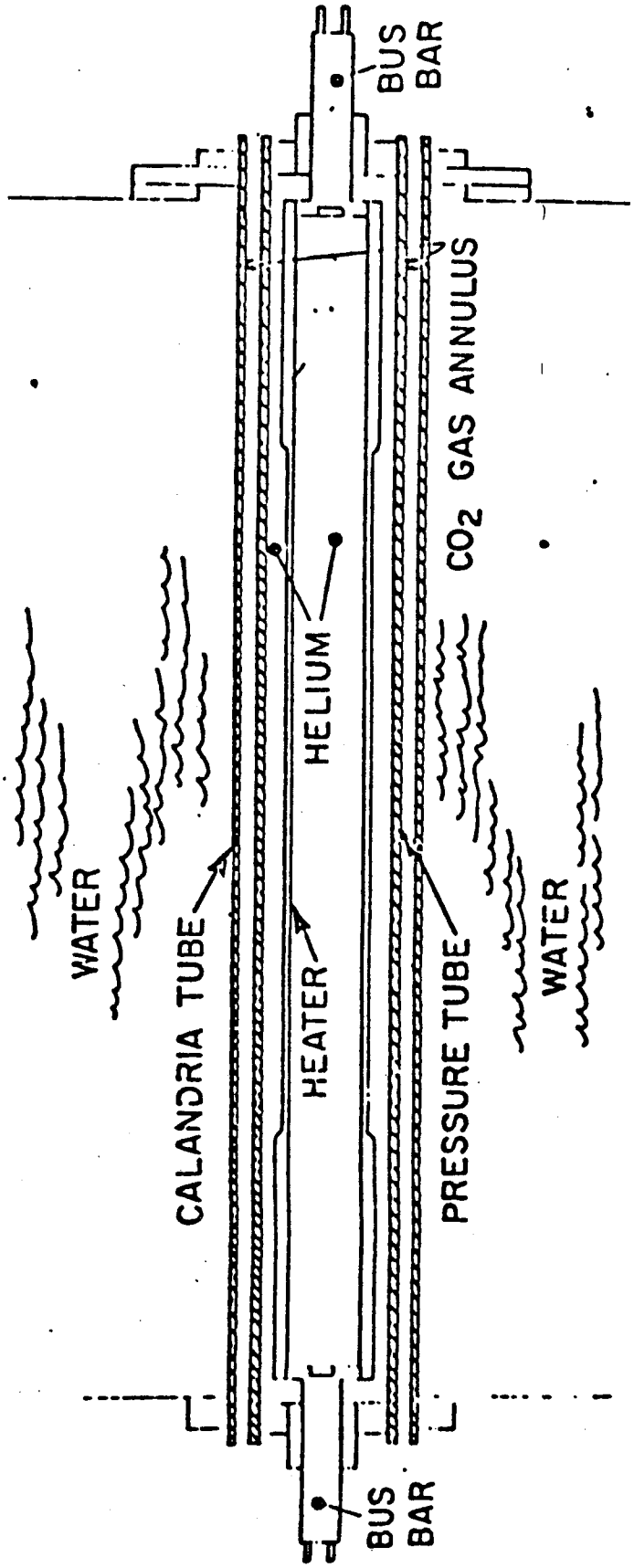

FIGURE 16.12 CONTACT BOILING EXPERIMENTAL SET-UP

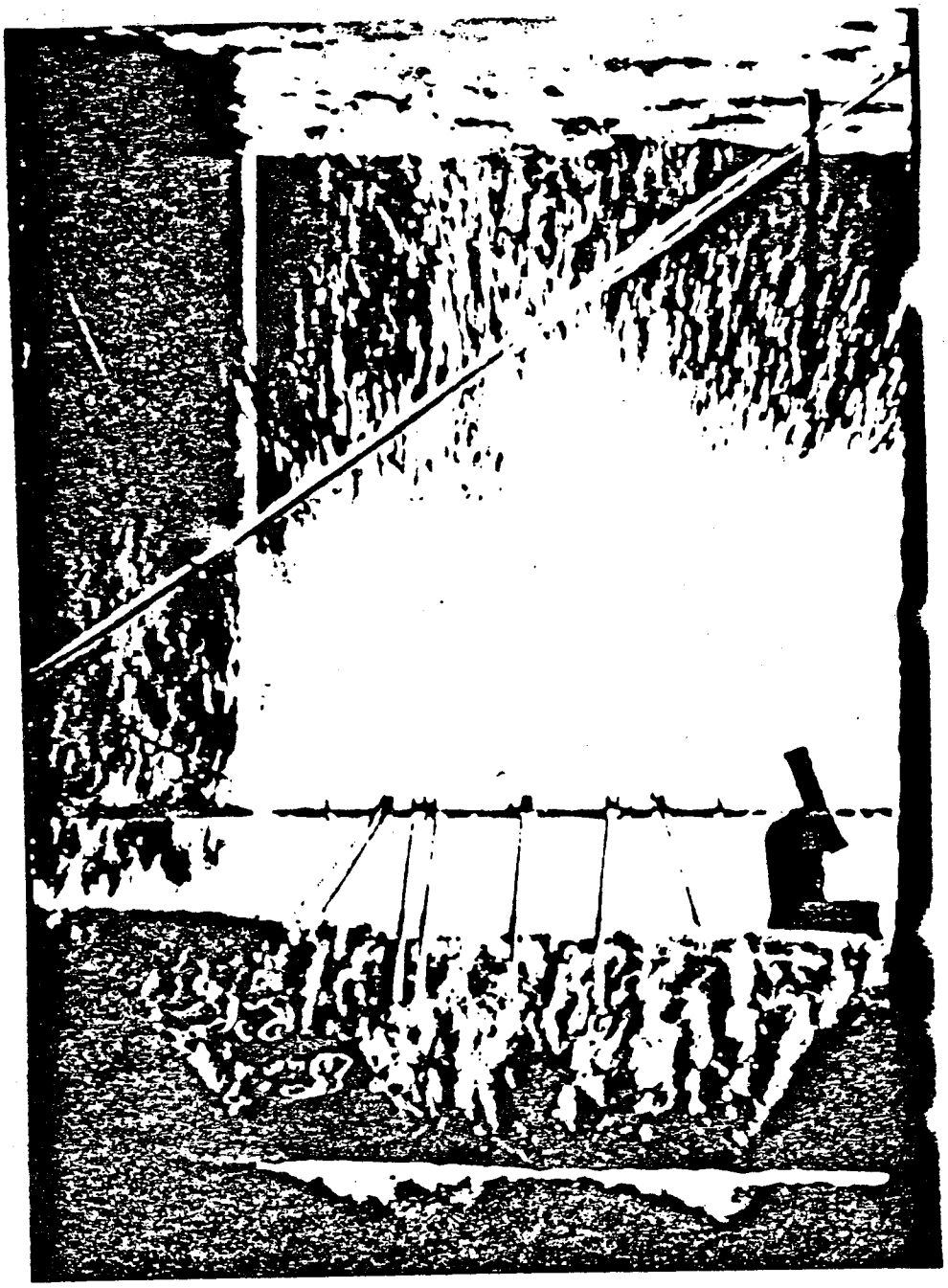

BOILING ON CALANDRIA TUBE: EXPERIMENT 4

FIGURE 16.13

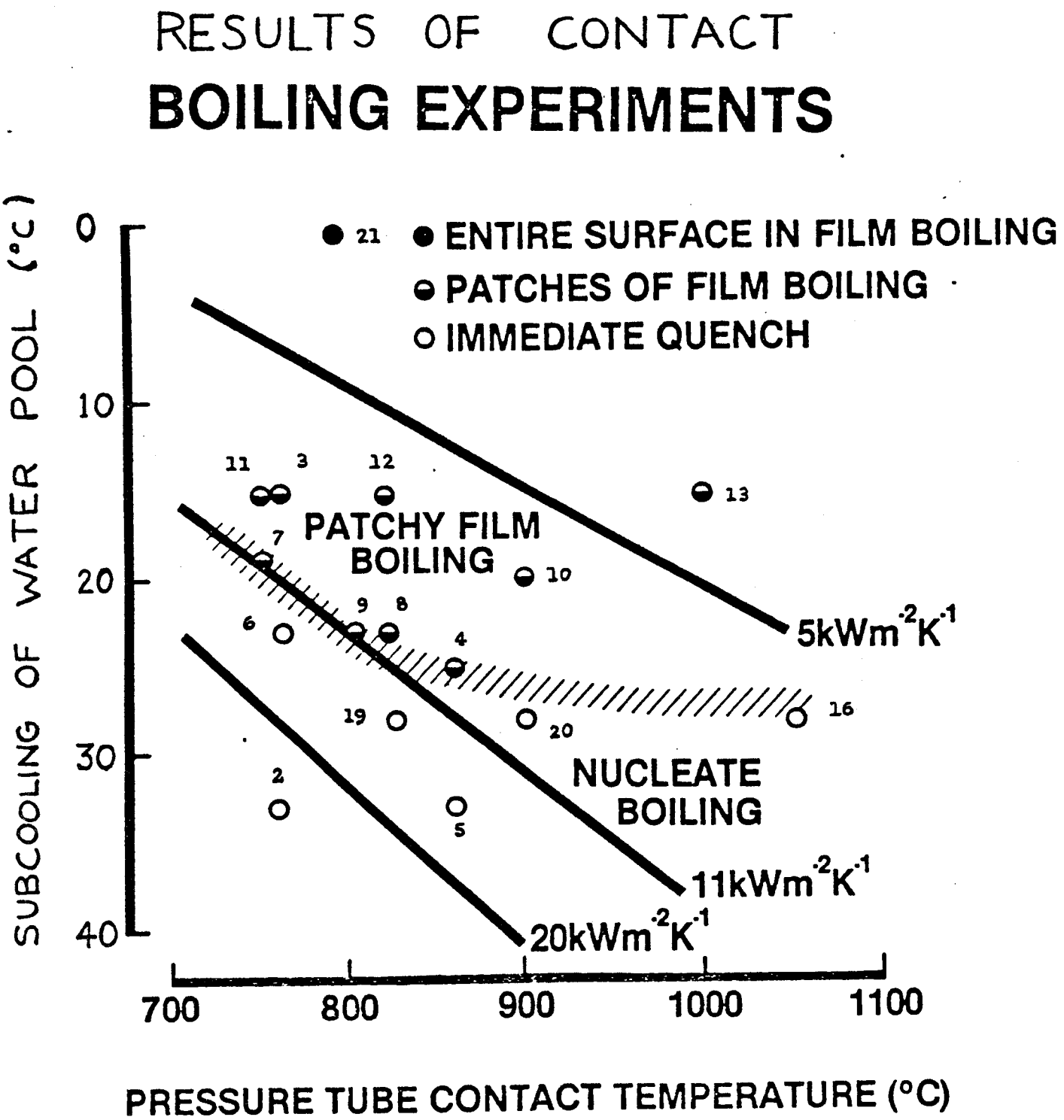
RESULTS OF CONTACT
BOILING EXPERIMENTS
SUBCOOLING OF WATER POOL (°C)
0
10
20
30
40
21
ENTIRE SURFACE IN FILM BOILING
PATCHES OF FILM BOILING
IMMEDIATE QUENCH
11
3
12
13
PATCHY FILM
BOILING
7
10
9
8
6
4
16
19
20
NUCLEATE
BOILING
2
5
5kWm-2K-1
11kWm-2K-1
20kWm-2K-1
700
800
900
1000
1100
PRESSURE TUBE CONTACT TEMPERATURE (°C)

FIGURE 16.14

CALANDRIA TUBE REWET

Caused by axial and circumferential conduction of heat from areas in Film Boiling to areas in Nucleate Boiling

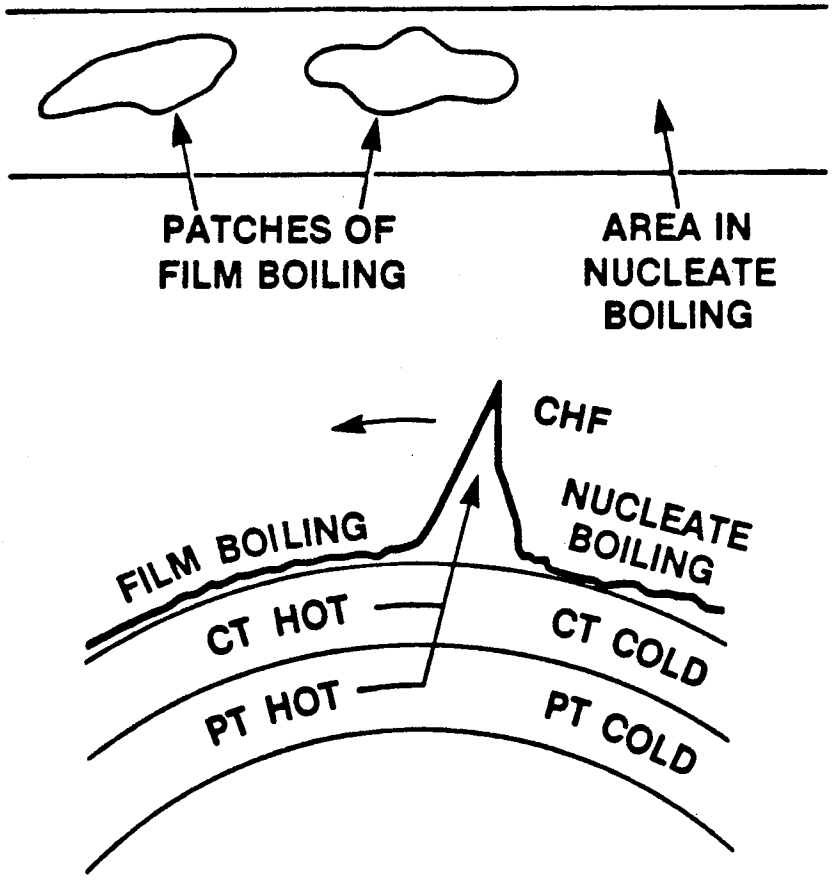

FIGURE 16.15

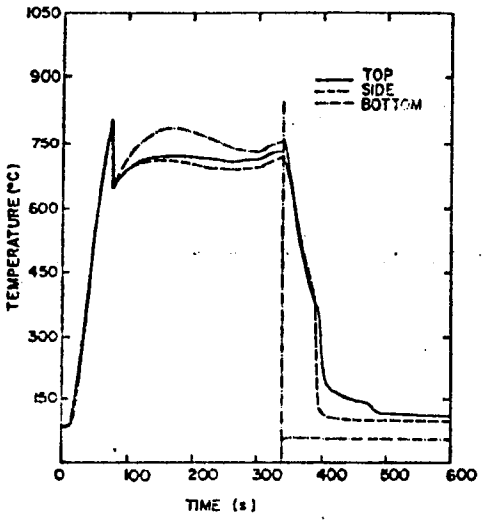

FIGURE a TIME VARIATION OF PRESSURE-TUBE TEMPERATURE

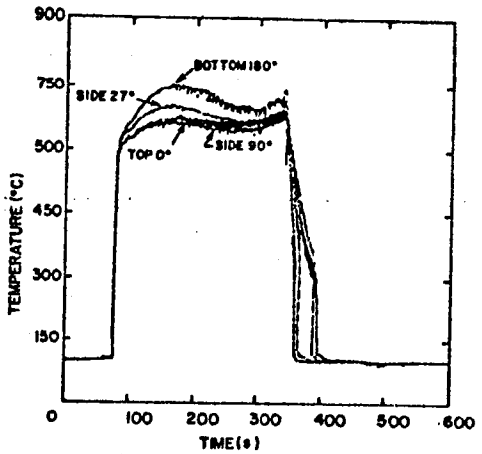

FIGURE b TIME VARIATION OF CALANDRIA-TUBE TEMPERATURE

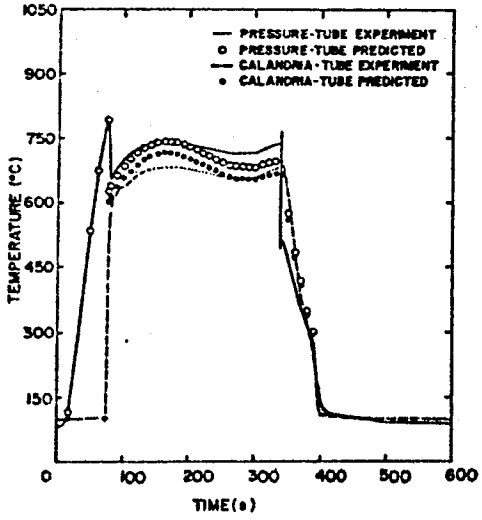

FIGURE c COMPARISON OF EXPERIMENTAL RESULTS WITH PREDICTIONS

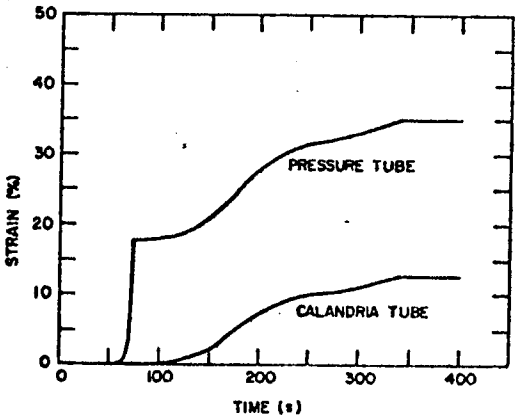

FIGURE d PREDICTED STRAIN

FIGURE 16.16

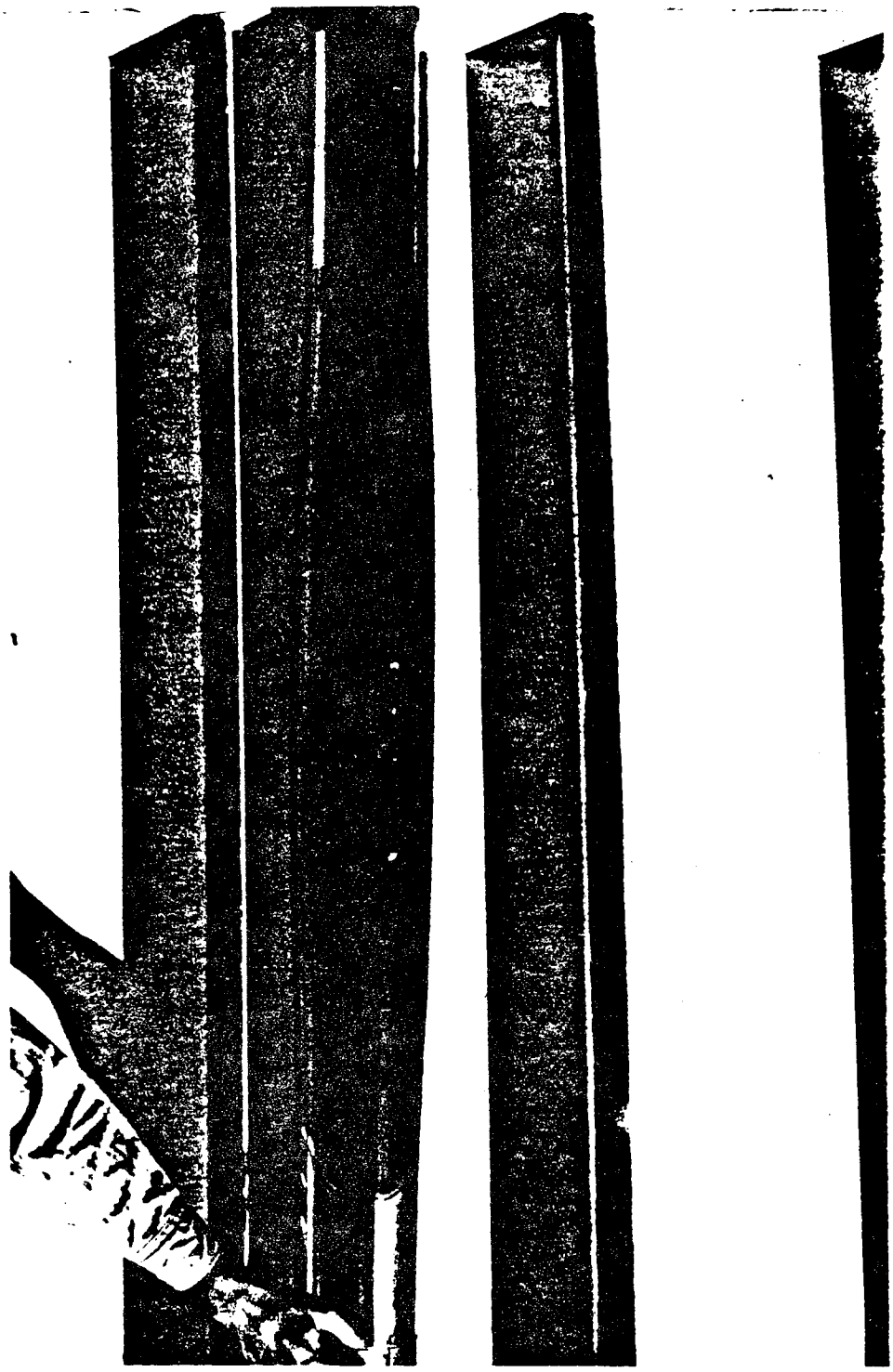

CONTACT BOILING TEST 21

FIGURE 16.17

METHODOLOGY

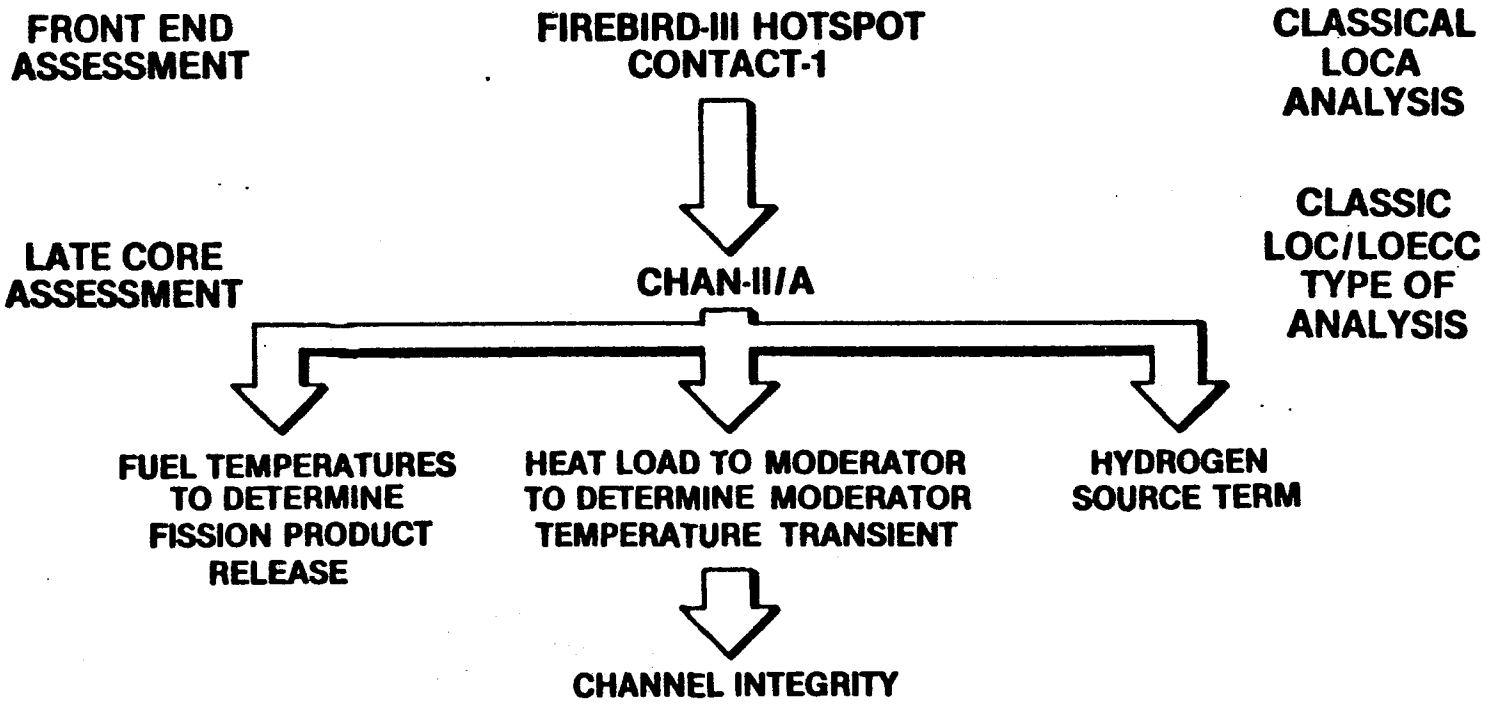

FIGURE 16.20

FIGURE 16.18

Large Scale Sag Test Rig

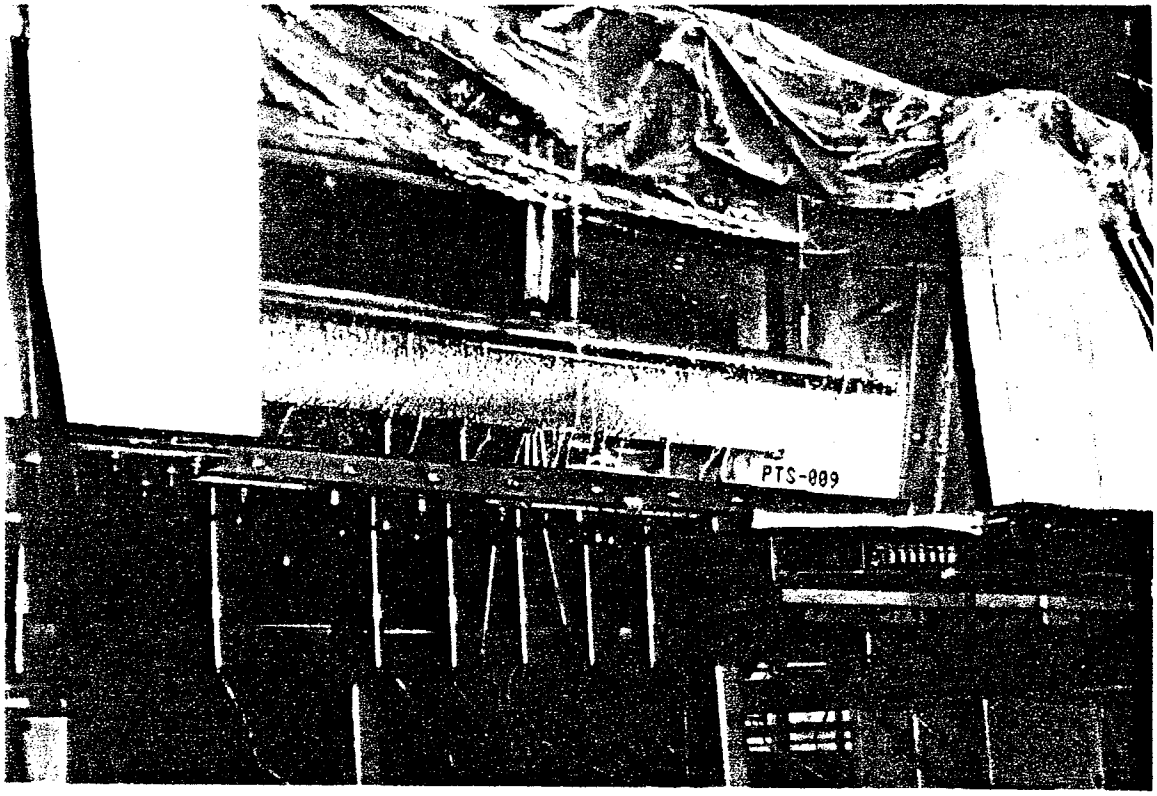

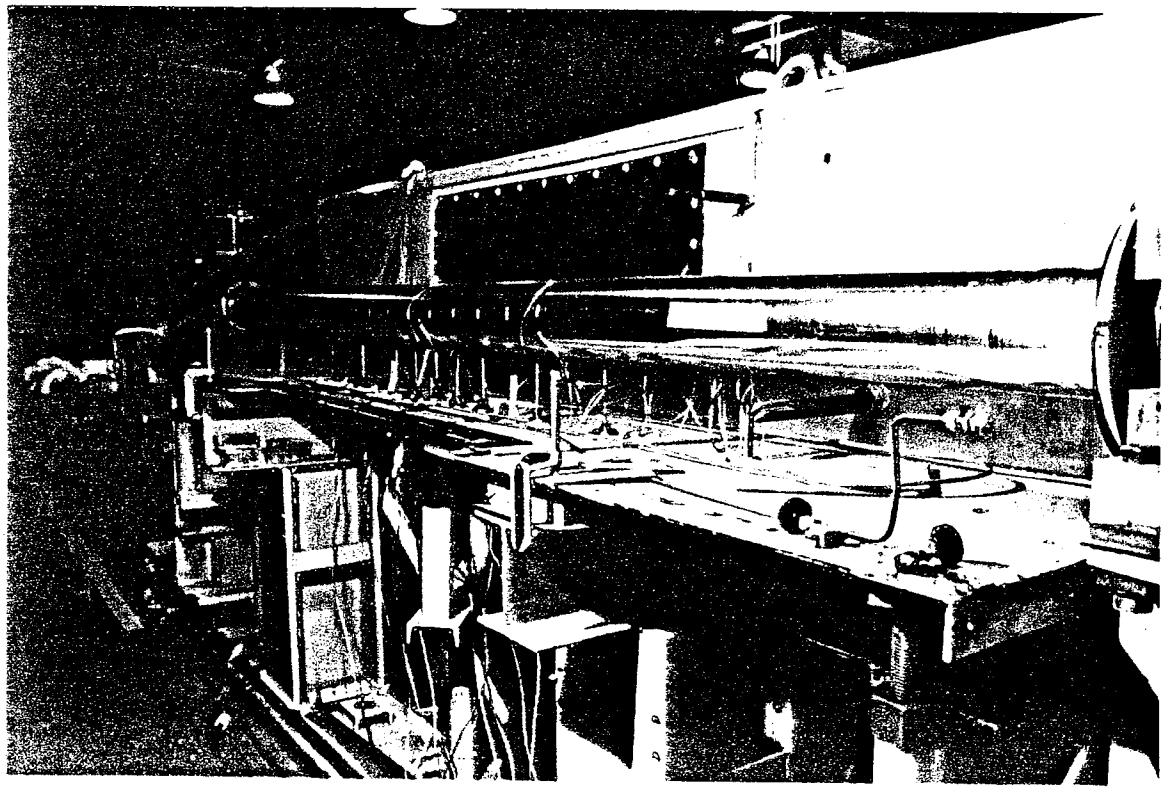

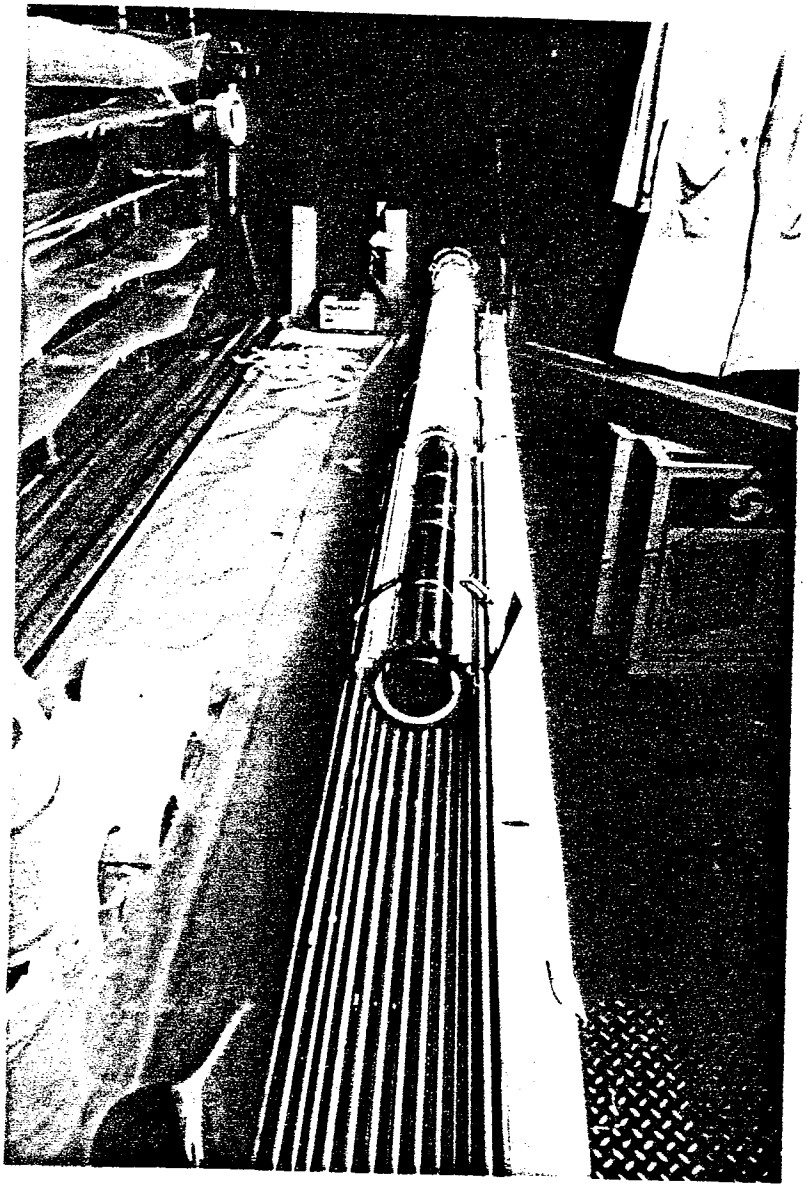

Heater Arrangement for Large Scale
Sag Experiments

FIGURE 16.19

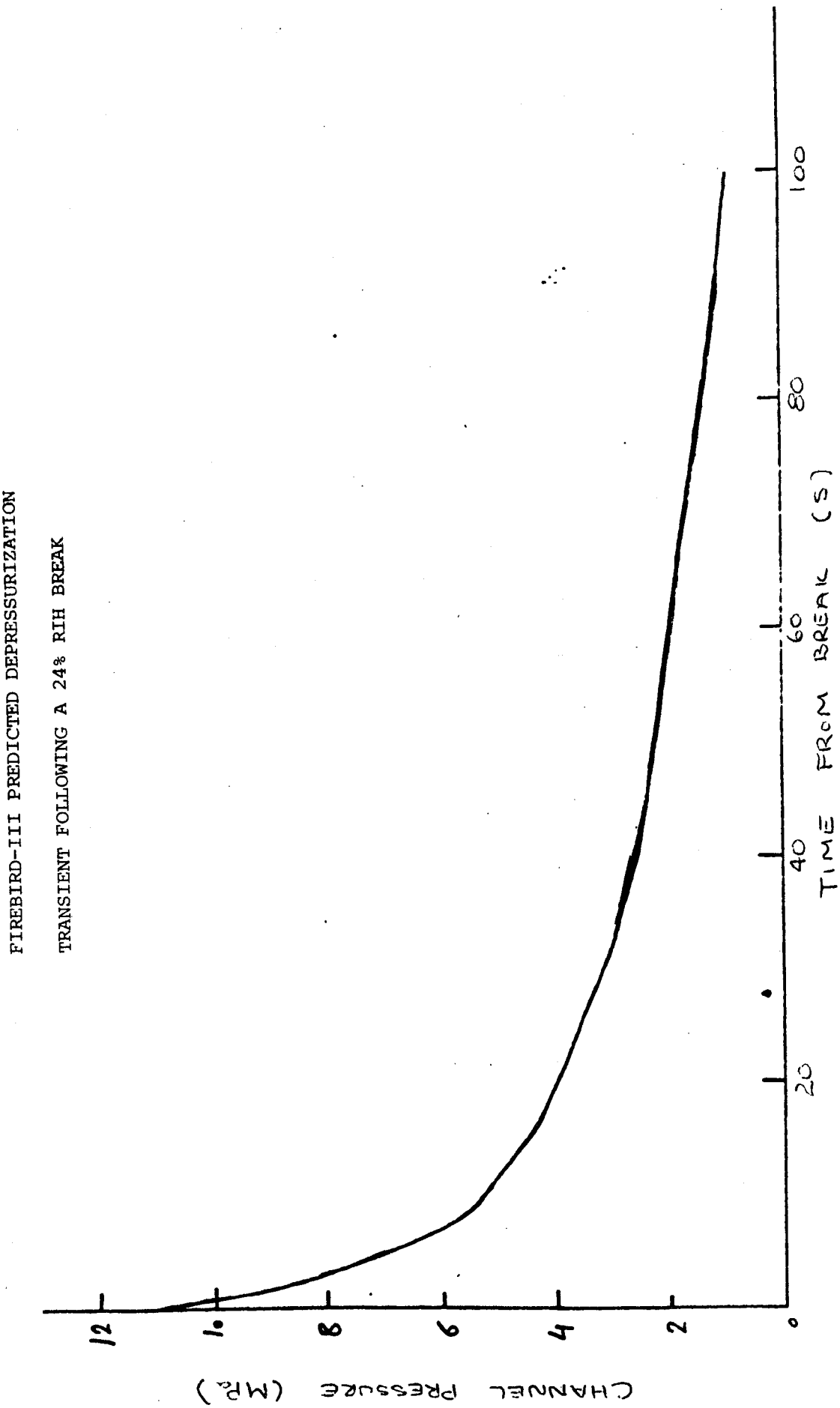
FIREBIRD-III PREDICTED DEPRESSURIZATION
TRANSIENT FOLLOWING A 24% RIH BREAK
CHANNEL PRESSURE (MPa)
12
10
8
6
4
2
0
20
40
60
80
100
TIME FROM BREAK (S)

FIGURE 16.21

CHAN-II (WNRE)

FUEL CHANNEL AND FEEDER ASSEMBLY

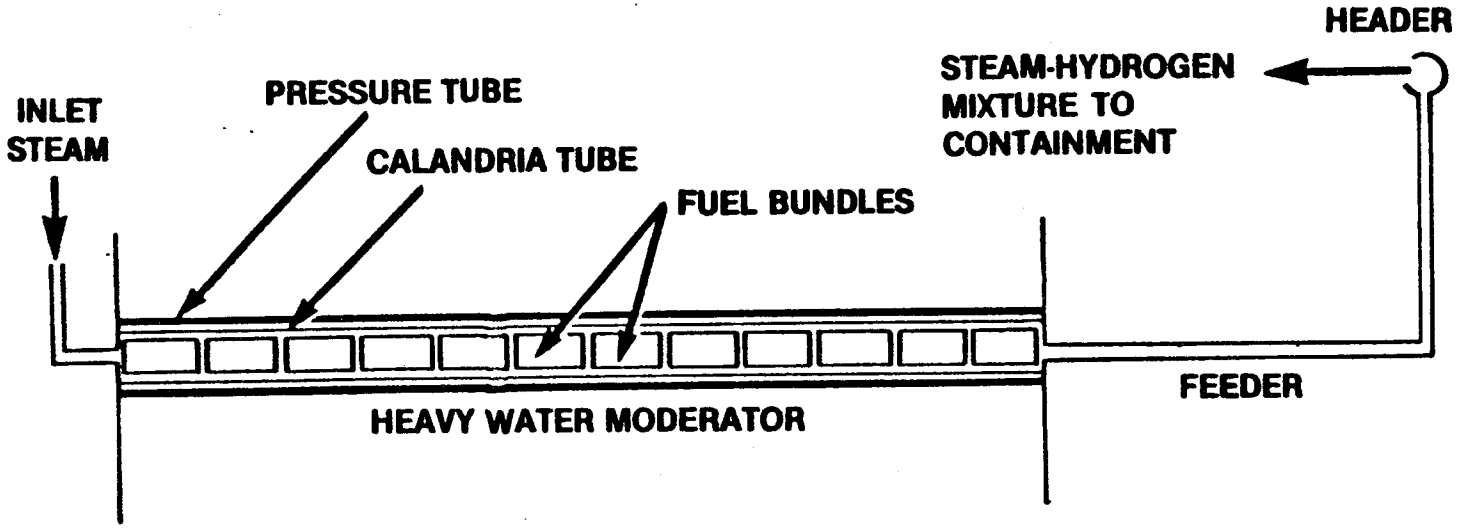

- Thermal radiation
- Metal water reaction

  $Zr + 2H_2O \rightarrow ZrO_2 + 2H_2 + E$
- Pressure tube sag

FIGURE 16.22

FUEL CHANNEL SEGMENT MODEL BEFORE CONTACT

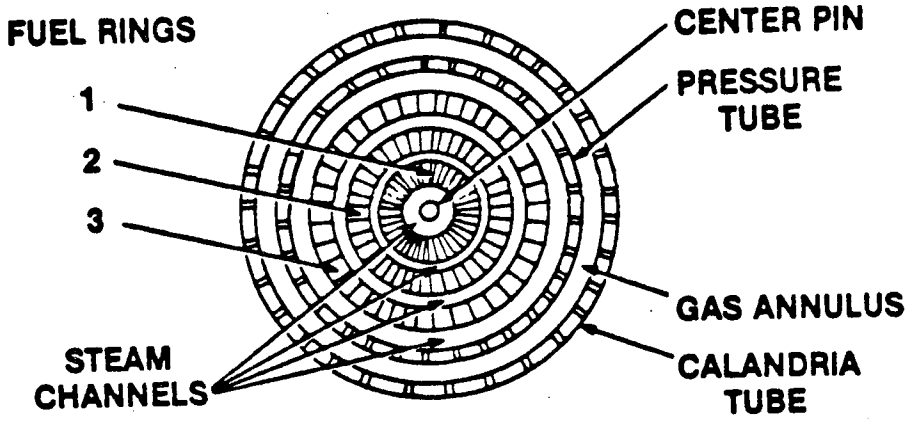

FUEL CHANNEL SEGMENT MODEL AFTER CONTACT

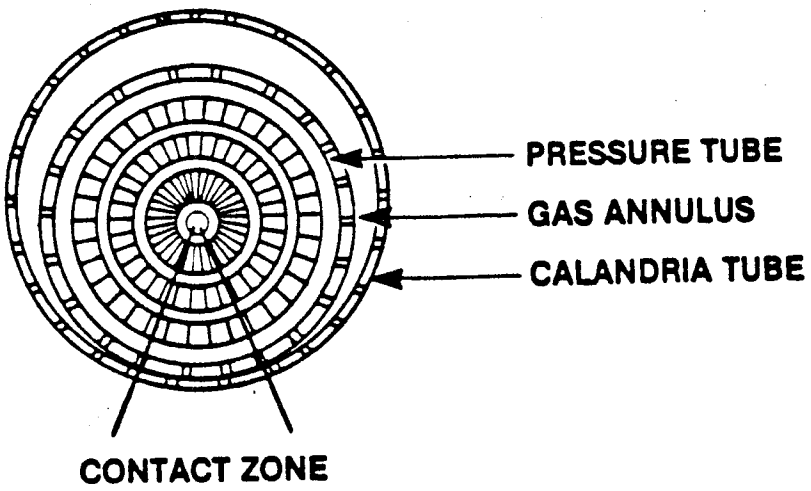

FIGURE 16.23

HYDROGEN PRODUCED FROM END OF BLOWDOWN vs STEAM FLOWRATE TO EACH CHANNEL

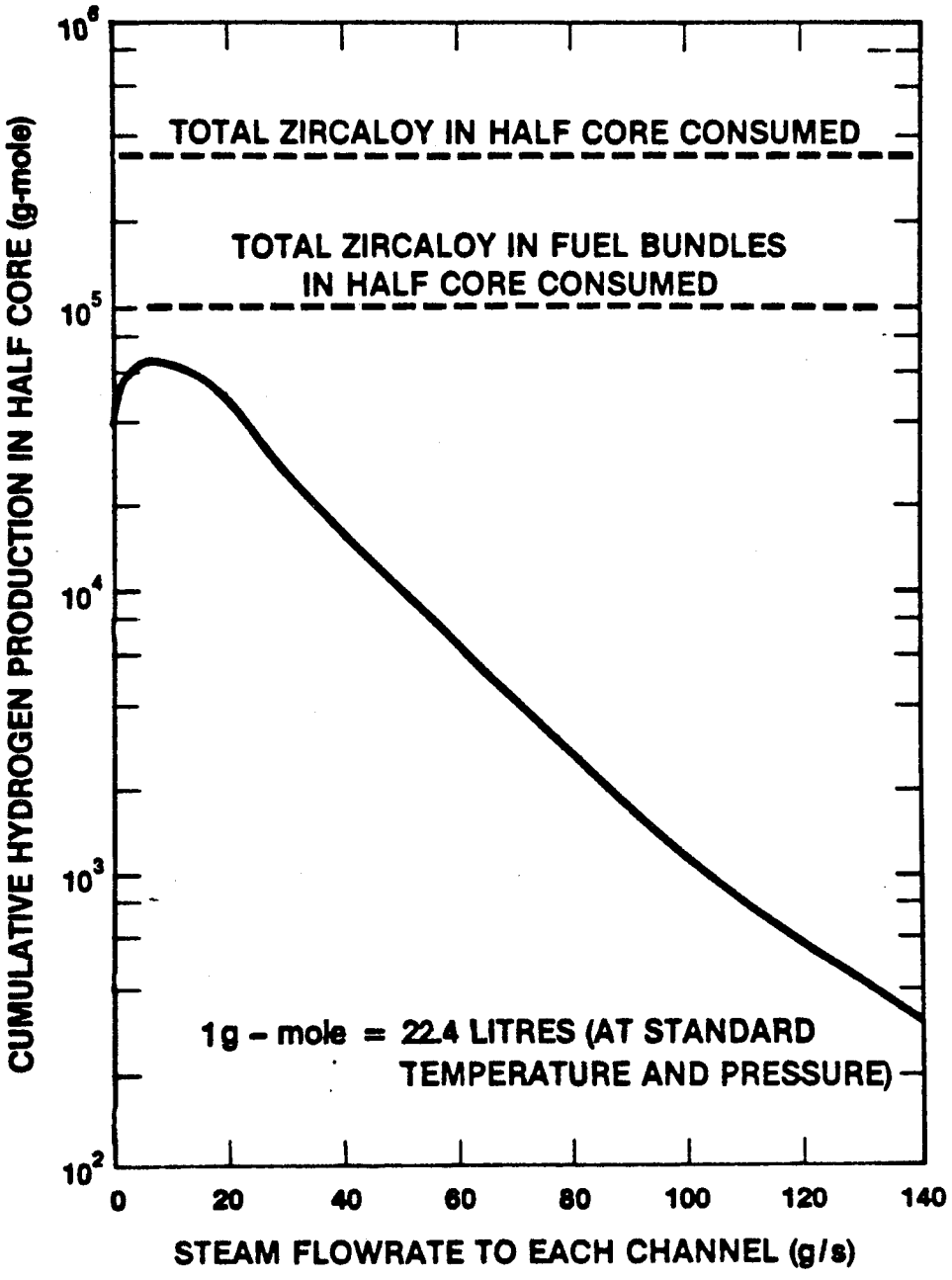

FIGURE 16.24

EFFECT OF STEAM FLOW RATE ON HYDROGEN PRODUCTION

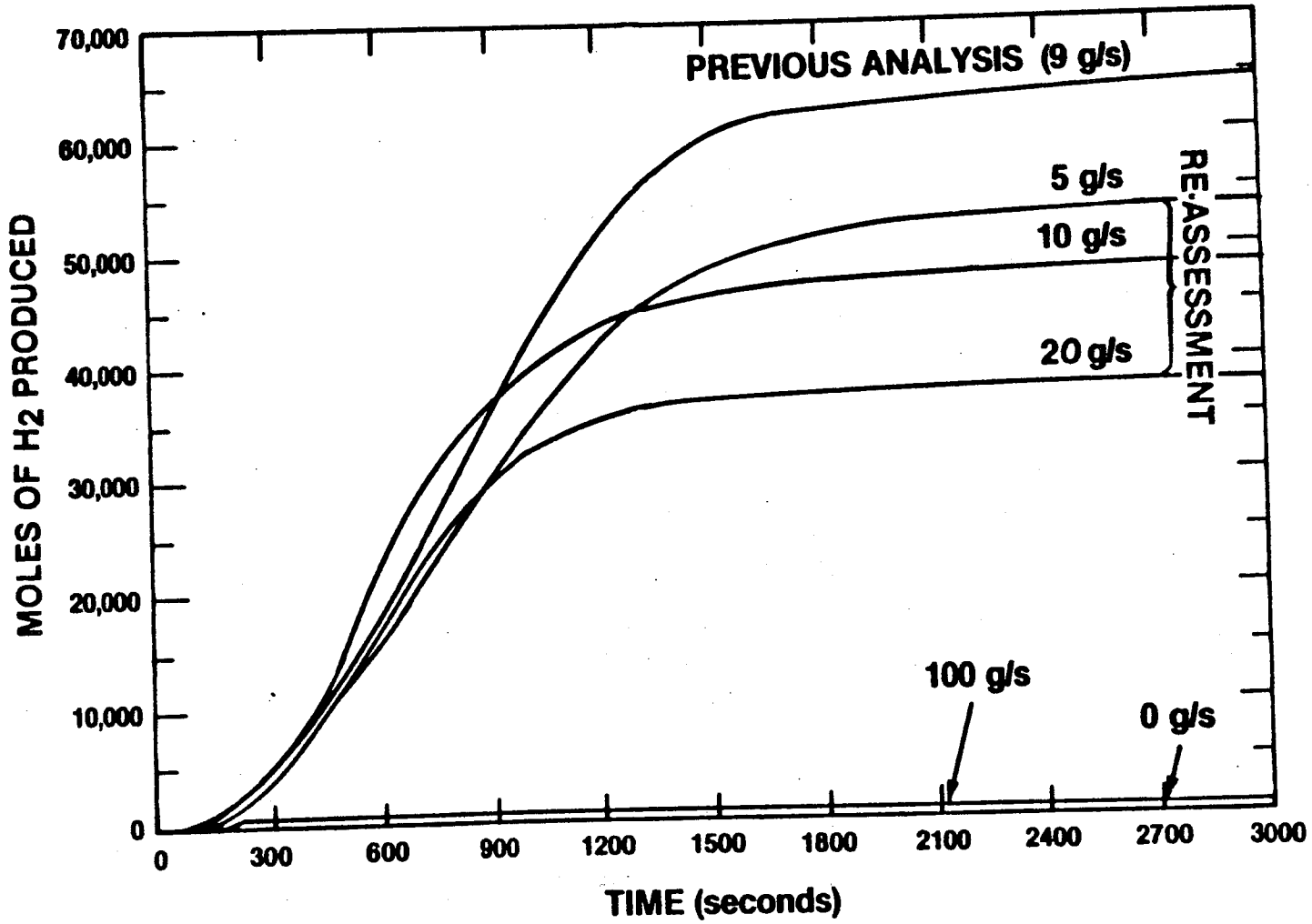

FIGURE 16.25

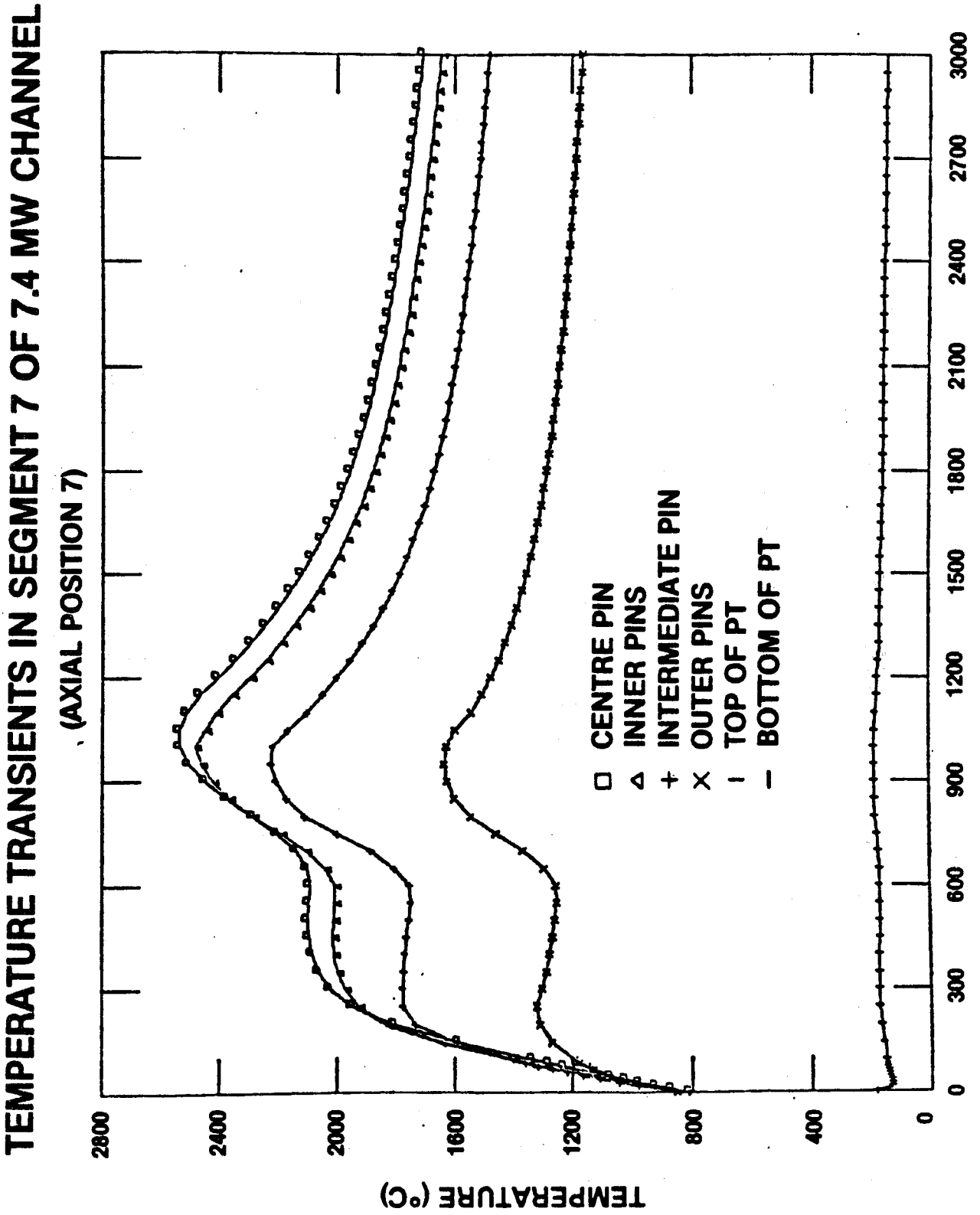
TEMPERATURE TRANSIENTS IN SEGMENT 7 OF 7.4 MW CHANNEL
(AXIAL POSITION 7)
TEMPERATURE (°C)
2800
2400
2000
1600
1200
800
400
0
0
300
600
900
1200
1500
1800
2100
2400
2700
3000
TIME AFTER BLOWDOWN (seconds)
CENTRE PIN
INNER PINS
INTERMEDIATE PIN
OUTER PINS
TOP OF PT
BOTTOM OF PT

FIGURE 16.26

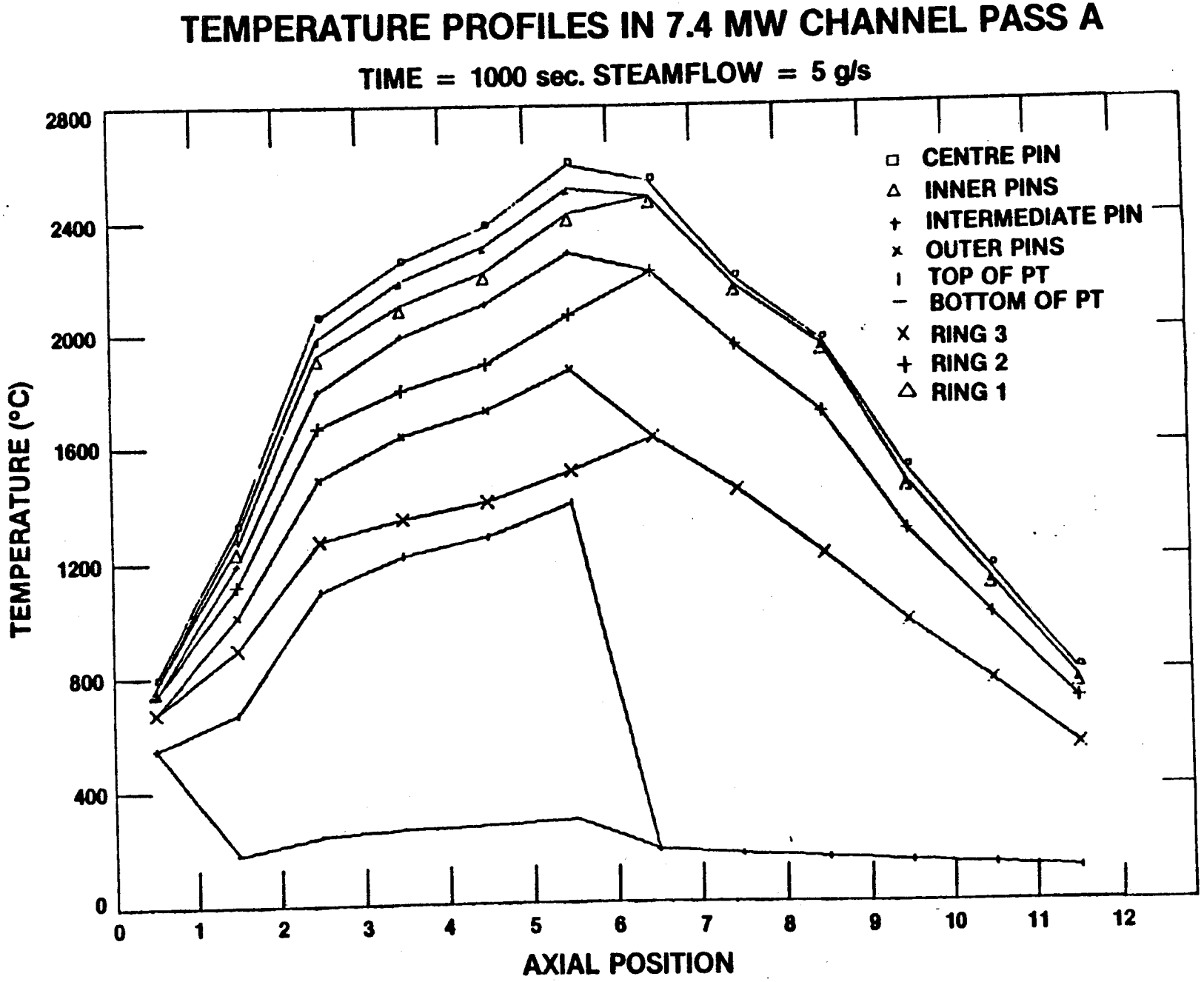
TEMPERATURE PROFILES IN 7.4 MW CHANNEL PASS A
TIME = 1000 sec. STEAMFLOW = 5 g/s
TEMPERATURE (°C)
2800
2400
2000
1600
1200
800
400
0
0
1
2
3
4
5
6
7
8
9
10
11
12
AXIAL POSITION
CENTRE PIN
INNER PINS
INTERMEDIATE PIN
OUTER PINS
TOP OF PT
BOTTOM OF PT
RING 3
RING 2
RING 1

FIGURE 16.28

TEMPERATURE TRANSIENTS IN SEGMENT 7 OF 4.8 MW CHANNEL

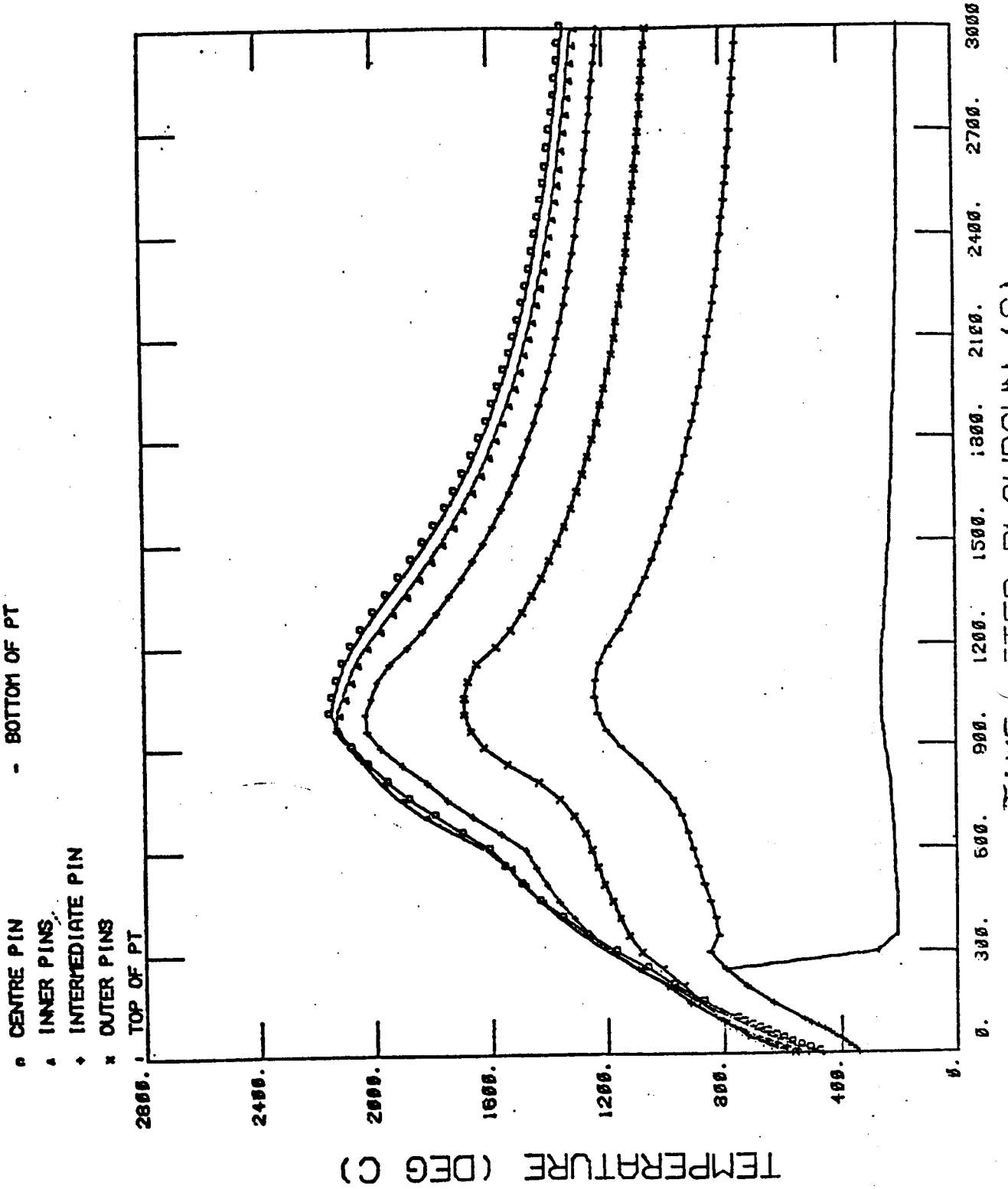

MODERATOR TEMPERATURE DISTRIBUTIONS

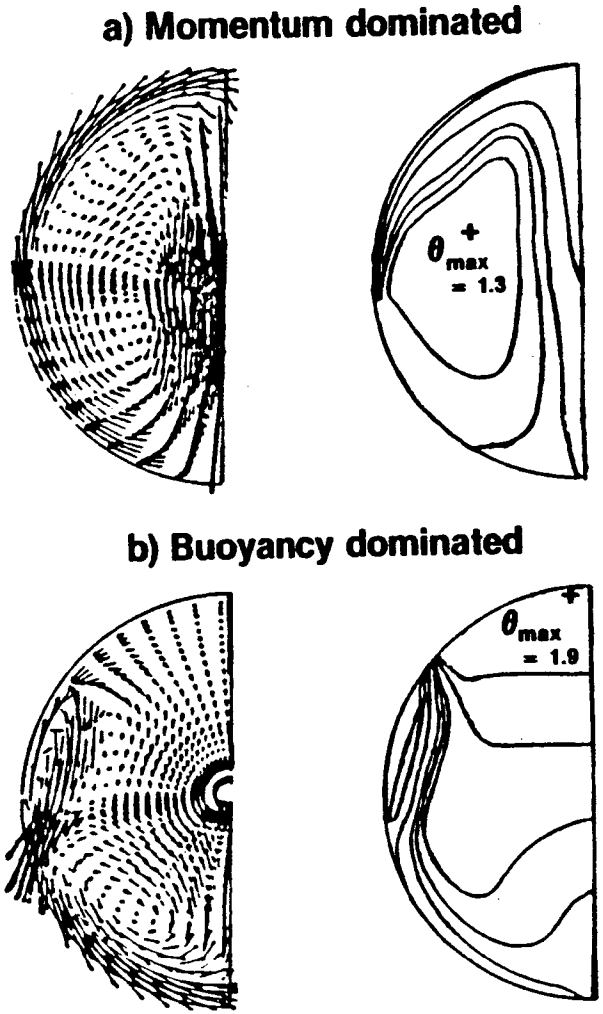

FIGURE 16.29

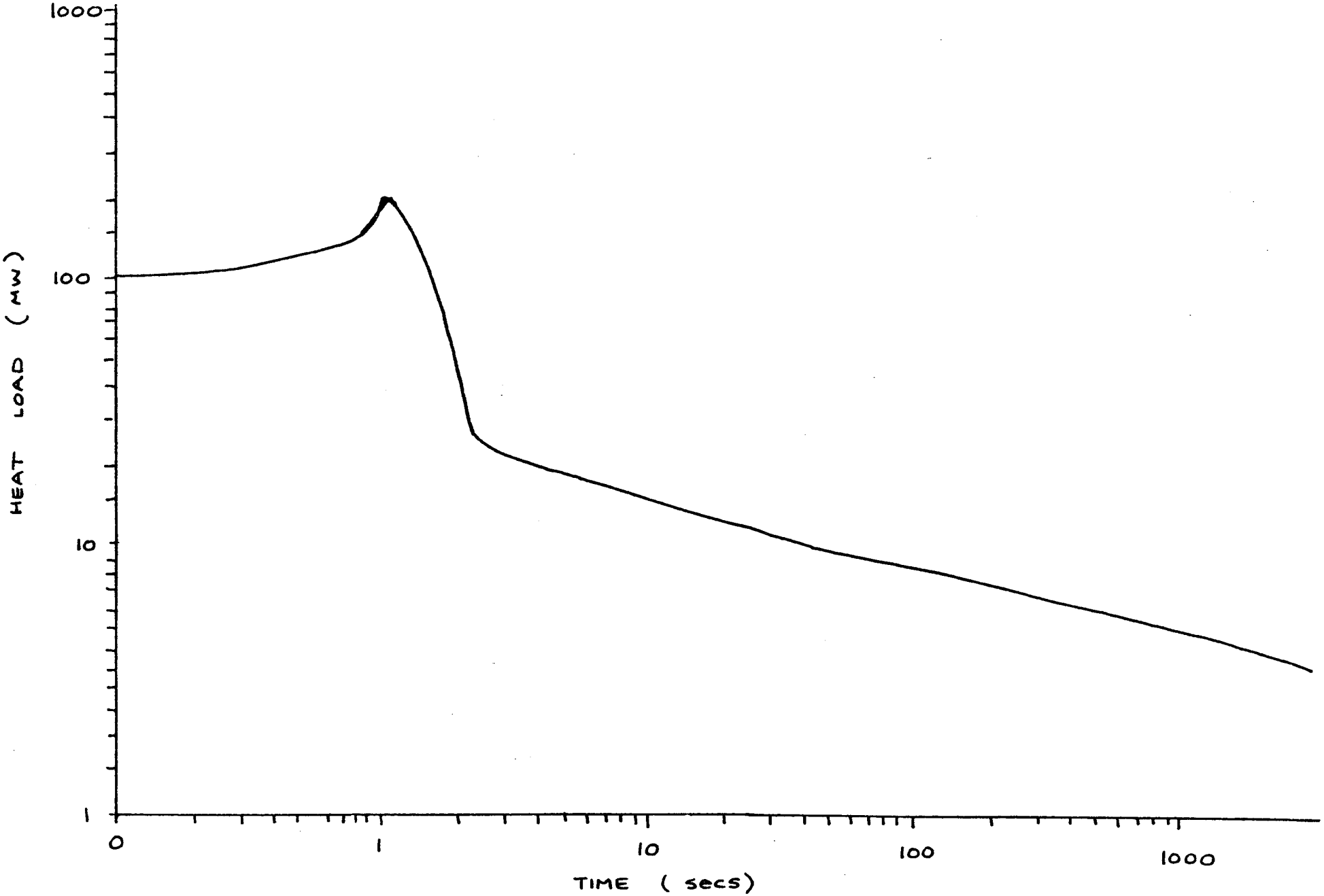

FIGURE 16.30 n-γ HEAT LOAD TO MODERATOR FOLLOWING 24% RIH BREAK (LOG-LOG SCALE)

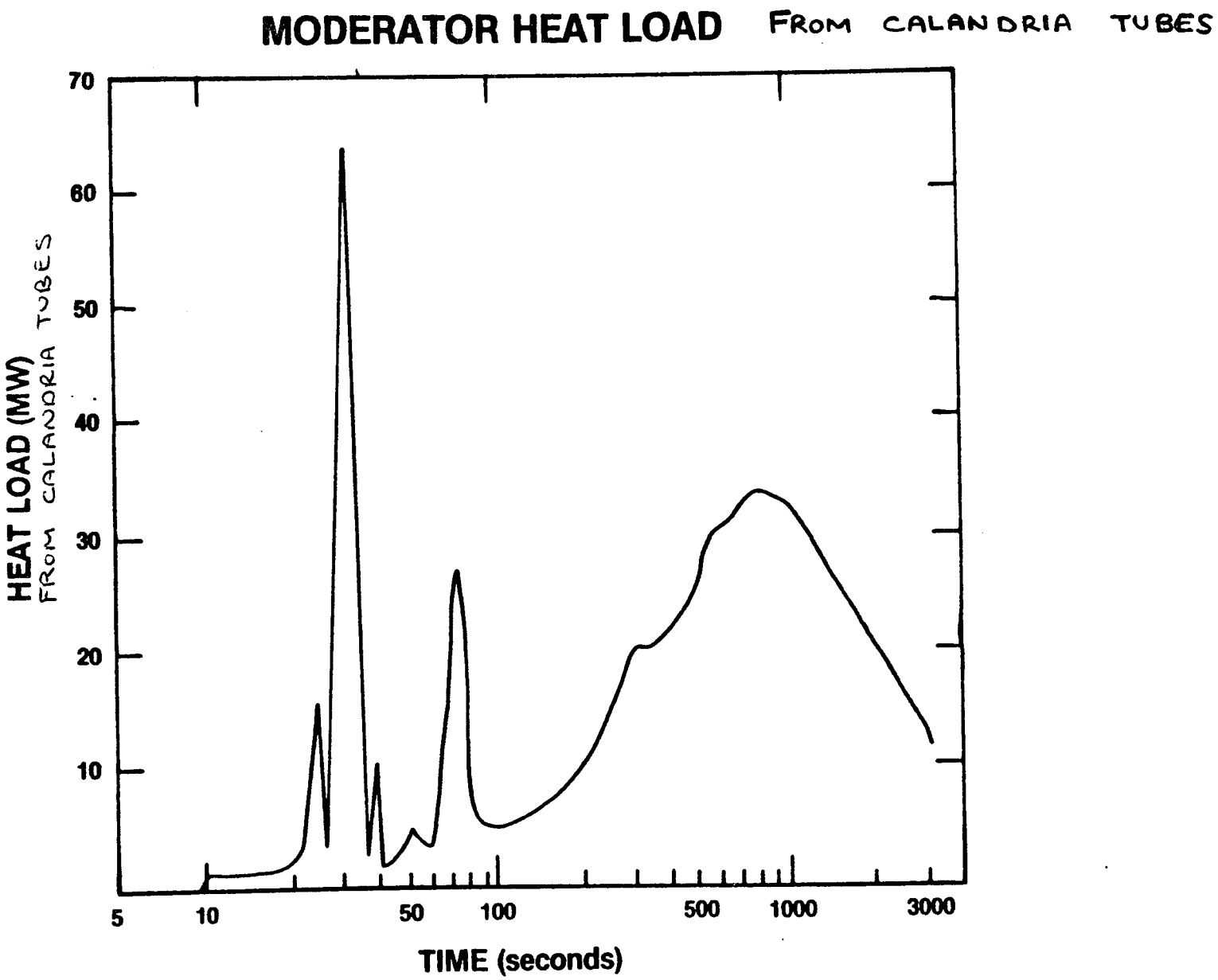
MODERATOR HEAT LOAD FROM CALANDRIA TUBES
HEAT LOAD (MW)
FROM CALANDRIA TUBES
70
60
50
40
30
20
10
5
10
50
100
500
1000
3000
TIME (seconds)

FIGURE 16.31